Synthesis and Characterization of Nickel Ferrite / CNFs Nano hybrid

By

Syeda Aatika Atique

School of Chemical and Materials Engineering (SCME)
National University of Sciences and Technology (NUST)
2017

Synthesis and Characterization of Nickel Ferrite / CNFs Nano hybrid

Name: Syeda Aatika Atique
Reg. No: NUST201362933MSCME67913F

This thesis is submitted as a partial fulfillment of the requirements for the degree of

MS in Nanoscience and Engineering

Supervisor Name: Dr. Iftikhar Hussain Gul

School of Chemical and Materials Engineering (SCME)

National University of Sciences and Technology (NUST)

H-12 Islamabad, Pakistan

January, 2017

Certificate

This is to certify that work in this thesis has been carried out by **Ms. Syeda Aatika Atique** and completed under my supervision in Thermal Transport Laboratory, School of Chemical and Materials Engineering, National University of Sciences and
Technology, H-12, Islamabad, Pakistan.

Supervisor: _____

Prof. Dr. Iftikhar Hussain Gul

Thermal Transport Laboratory
Material Engineering Department
National University of Sciences
and Technology,
Islamabad

Submitted through

Principal/Dean,
School of Chemicals and Materials Engineering Department
National University of Sciences and Technology, Islamabad

Dedication

I would like to dedicate this thesis to my beloved father

Syed M. Atique-Ur-Rehman Gilani.

Acknowledgements:

In the name of Allah, the Most Gracious and the Most Merciful. First of all, I would like to express my gratitude to the one, who deserves the most, all praise to almighty Allah, the most beneficent, the creator of the universe, who enabled me to complete this research work successfully.

Millions of blessings on Prophet Muhammad (S.A.W), who dedicated his whole life for the betterment of mankind, served as true torch-bearer towards the path of success and his preachings have always proved to be the source of inspiration and guidance in every field of life for all of us.

I wish to express my sincere thanks to; Principal of the SCME and HOD Materials Engineering for providing me with all the necessary facilities for the research. I feel privileged to have the honor to acknowledge my research supervisor Dr. Iftikhar Hussain Gul to whom I owe my indescribable special indebtedness, who was very affectionate and cooperative during entire research work. Without his kind and sincere efforts it might have not been possible for me to end this work in time.

I offer my special and sincere thanks to my Lab Fellows; Ms. Anum Rabab (Internee), Mr. Hashim Naseer (MS-Scholar), Mr. Sumair Ahmed Soomro (MS-Scholar), Mr. Allah Bakhsh (PhD-Scholar) and Mr. Muhammad Zarrar Khan (PhD-Scholar) who guided me through the rough patches and helped me in completing my research project.

My Sincere regards to our Lab Attendants Mr. Zafar Iqbal, Mr. Khurram, Mr. Shams and all other department faculty members who were always there to help me and support me to finish my practical work in time.

Finally, I wish to offer my humble gratitude to my great father Syed M.Atique-ur-Rehman, my husband Syed Anwar Alam Gilani, my brother Syed Sami-ur-Rehman and my beloved sister for their unceasing encouragement, prayers, material and moral support in every sphere of my life that paved the way for me to reach this destination.

Finally the last but not the least, I am forever indebted to my late mother, who taught me about values in my early childhood. Her words of wisdom and prayers will forever be a source of encouragement for the rest of my life. May Allah rest her soul in peace and make her stay in Jannat-ul-Firdous. I have realized that in my whole life, God blessed me just because of the support and prayers of my family.

It's all thanks to their affection, love and prayers I received from the above mentioned people, guiding me constantly in this world.

Sincerely,

Syeda Aatika Atique Gilani

Abstract:

Nickel ferrite was prepared by wet chemical co-precipitation method. Carbon nanofiber was well dispersed in Nickel ferrite by the use of polar solvent ortho- Xylene. Novel one step method was used to synthesize different compositions of $NiFe_2O_4$/CNF nanohybrid, where CNF concentration was continuously increased (0%,10%,15% and 20% by weight) . The nanohybrid synthesis was confirmed by employing characterization techniques like X-Ray Diffraction (XRD), Fourier Transform Infrared Spectroscopy (FTIR), Scanning Electron Microscope (SEM) and dielectric properties were studied using impedance analyser techniques. XRD patterns confirmed the formation of $NiFe_2O_4$/CNF nanohybrid with crystallite size in the range of 28±4 nm, decreasing bulk density, x-ray density and increasing porosity. FTIR patterns show two characteristic absorption bands and confirms that carbon nanofiber did not interfered with spinel structure of nickel ferrite. SEM images confirmed the complete coating of nickel ferrite nanoparticles on carbon nanofiber and efficiency of our described novel method. The dielectric properties: dielectric constant, dielecric loss, tangent loss and AC conductivity showed huge enhancement with increase in CNF weight percent. Pure $NiFe_2O_4$ showed dielectric constant of 1.79×10^3 at 100 Hz while it was increased massively to 2.92×10^6 at 100 Hz for 20% addition of CNF, which renders this nanohybrid to have potential applications as supercapacitors. The impedance analysis showed the considerable decrease of resistance, reactance and cole-cole plot on the addition of carbon nanofibers. For example: The pure $NiFe_2O_4$ has highest impedance values of 3.67×10^7 Ohm at 100 Hz and $NiFe_2O_4$ /CNF nanohybrid with 20% CNFs concentration has the lowest impedance values of 1.38×10^7 Ohm at 100 Hz, which proves this nanohybrid useful for high frequency applications and microwave absorbing appliances.

Table of Contents

Chapter 1: Introduction

Sr. No.	Title	Page No.
1.1	Nanotechnology	1
1.1.1	Top-down approach	1
1.1.2	Bottom-up approach	2
1.2	Applications of Nanomaterials	3
1.3	Magnetic Materials	3
1.3.1	Soft Magnetic materials	3
1.3.2	Hard Magnetic materials	4
1.4	Types of Magnetic materials	4
1.4.1	Dia-magnetic	4
1.4.2	Para-magnetic	5
1.4.3	Ferro-magnetic	6
1.4.4	Ferri-magnetic	7
1.4.5	Anti-ferromagnetic	7
1.4.6	Super-paramagnetic	8
1.5	Ferrites	8
1.5.1	Soft Ferrites	9
1.5.2	Hard Ferrites	9
1.6	Types of Ferrites	9
1.6.1	Spinal Ferrites	9
1.6.1.1	Tetrahedral sites	10
1.6.1.2	Octahedral sites	10
1.6.1.3	Types of Spinel Ferrites	10
1.6.2	Garnet Ferrites	12
1.6.3	Hexagonal Ferrites	12
1.7	Nickel Ferrites	13
1.8	Application of Ferrites	13
1.9	Introduction to Carbon Nanofibers (CNFs)	14
1.9.1	Applications of CNFs	15
1.9.2	Advantages of using CNFs	16
1.10	Nanohybrid of $NiFe_2O_4$ / CNFs	16
1.11	Objectives	19

Chapter 2: Theoretical Review

Sr. No.	Title	Page No.
2.1	Synthetic approaches of nanoparticles	20
2.2	Synthesis Techniques of nanoparticles	20
2.3	Chemical Co-precipitation method	21
2.3.1	Main steps in Co-precipitation method	23
2.3.1.1	Co-precipitation step	23
2.3.1.2	Ferritisation step	24
2.3.2	Factors upon which Co-precipitation depends	24
2.2.1.1	Effect of pH	25
2.3.1.2	Effect of temperature	25
2.3.1.3	Mixing rate of the reactants	25
2.3.1.4	Role of Cations	25
2.3.1.5	Heating after Co-precipitation	25
2.3.1.6	Advantages of Co-precipitation method	26
2.4	Synthesis of $NiFe_2O_4$	26
2.5	Xylene as a Dispersive Medium	27
2.6	Synthesis of $NiFe_20_4$ / CNFs Nanohybrid	28
2	Summary of Experimental work	29

Chapter 3: Introduction to Sample Characterization Techniques

Sr. No.	Title	Page No.
3.1	Introduction	30
3.2	X-Ray Diffraction technique	31
3.2.1	Working principle of XRD	31
3.2.2	Lattice Constant	33
3.2.3	Crystallite Size	34
3.2.4	X-Ray Density	35
3.2.5	Bulk Density	35
3.2.6	Porosity Fraction	35
3.3	Fourier Transform Infrared Spectroscopy	36
3.3.1	Working principle of FT-IR	36
3.4	Scanning Electron Microscopy	37
3.4.1	Working principle of SEM	38
3.5	Dielectric Properties	40
3.6	AC Conductivity	40

3.7 AC Impedance Spectroscopy 41

Chapter 4: Results and Discussions:

Sr. No.	Title	Page No.
4.1	X-ray Diffraction	42
4.2	Scanning Electron Microscopy	48
4.3	Fourier Transform Infrared Spectroscopy	52
4.4	Dielectric Properties	53
4.5	AC Conductivity	56
4.6	AC Impedance Spectroscopy	58
	Conclusion	62
	Future Work	62
	References	63

List of Figures

Chapter 1: Introduction

Fig. No.	Title	Page No.
1.1	Flow chart of top-down and bottom-up approach.	2
1.2	Diamagnetic material	5
1.3	Paramagnetic material	6
1.4	Ferromagnetic material and Ferrimagnetic material	6
1.5	Anti-ferromagnetic material	7
1.6	Super-paramagnetic material	8
1.7	Spinel ferrite unit cell with octahedral and tetrahedral sites	11
1.8	Carbon nanofibers	14
1.9	Cross sectional view of CNFs	15
1.10	Dielectric dipole orientation in the capacitor	17

Chapter 2: Theoretical Review

Fig. No.	Title	Page No.
2.1	Steps for the process of Chemical Co-precipitation	22
2.2	Isomers of Xylene	27
2.3	Summary of Experimentation	29

Chapter 3: Introduction to Sample Characterization Techniques

Fig. No.	Title	Page No.
3.1	Scattering of incident beams of x-rays at the plane of atoms	32
3.2 a	Reflection plane satisfying Bragg's law	33
3.2 b	Diffracted cone of radiations in powder method	33
3.3	Unit cell showing lattice constants	34
3.4	FT-IR equipment	36

3.5	Basic working principle of FTIR	37
3.6	Type of signals emitted from interaction volume	38
3.7	Basic principle of SEM	39

Chapter 4:
Results and Discussion

Fig. No.	Title	Page No.
4.1	XRD of Ferrite (0.0% CNFs)	42
4.2	XRD of CNF	43
4.3	XRD of ferrite with increasing CNFs content	44-45
4.4	Trend of lattice constant	47
4.5	Tend of crystallite size	47
4.6	Trend of porosity fraction	48
4.7	Trend of bulk density	48
4.8	Trend of X-ray density	49
4.9	SEM image for pure nickel ferrite	50
4.10	SEM image of pure CNFs	50
4.11	SEM image for nanohybrid of 35000 X	51
4.12	SEM image for nanohybrid of 50000 X	51
4.13	SEM image for nanohybrid of 80000 X	52
4.14	SEM image for nanohybrid of 100000 X	52
4.15	FT-IR spectra of pure Nickel ferrite & nanohybrid	53
4.16	Dielectric Constant as a function of frequency	55
4.17	Dielectric Loss Factor as a function of frequency	56
4.18	Tangent Loss Factor as a function of frequency	57
4.19	AC-Conductivity as a function of frequency	59
4.20	Impedance as a function of frequency	60
4.21	Trend of resistance (real part of impedance) with frequency	60
4.22	Trend of reactance (imaginary part of impedance) with frequency	61
4.23	Nyquist or Cole-Cole plot of AC Impedance	62

List of Tables

Chapter 1: Introduction

Table No.	Title	Page No.
1.1	Radii of some common metal ions used in the spinel ferrites	10
1.2	An overview of different types of spinel ferrites	12

Chapter 4: Results and Discussion

Table No.	Title	Page No.
4.1	Peak position of the reflection planes	43
4.2	Variation of average crystallite size, lattice parameter, molecular density, X-ray density, volume of cell and porosity	45
4.3	Tetrahedral (A) and octahedral (B) band positions for nanohybrid.	53
4.4	Variation of AC conductivity**,** dielectric tangent loss, dielectric constant, dielectric loss of nanohybrid.	57

Chapter 1

Introduction

1.1 Nano technology:

The branch of technology that deals with tolerances and dimensions of ranging from 1-100 nanometers, especially the manipulation of individual atoms and molecules. First time in on December 29, 1959, the Richard Feynman, a physicist who belonged to America lectured, "There's Plenty of Room at the Bottom," at meeting of an American Physical Society at Caltech. Then in 1974 conference, Norio Taniguchi, The scientist who belonged to Japan (Tokyo University of Science) used the term "nano-technology" for the very first time. After that in 1981 first paper on nanotechnology was published by Eric Drexler. The nano-technology progressed as a field due to the invention of scanning tunneling microscope in 1981.

In mid-2000's, United States of America started federal nanotechnology research and development program named as "The National Nanotechnology Initiative". The importance of nanotechnology was sensed immediately and all European countries allotted special funding for its development.

Two basic approaches were introduced for synthesis of nanomaterials, described as follows:

1.1.1 Top-down Approach:

The top-down approach as the name suggests often uses the concept of breaking big substances into smaller ones. Cutting, milling and shaping of materials is done by microfabrication methods or traditional workshop by the use of externally controlled tools to achieve the desired shape and order. The patterning techniques, such as inkjet printing and photolithography belong to this category. A new top-down approach, Vapor treatment has been introduced to engineer nanostructures.

1.1.2 Bottom up Approach:

Bottom up approach as the name refers to the making up of a nanomaterial from the bottom, from small to big materials i.e. atom by atom, molecule by molecule or cluster by cluster. For example: to synthesize nanoparticles, colloidal dispersion, self-assembly, deposition of film by chemical vapour growth are good examples of bottom up approach.

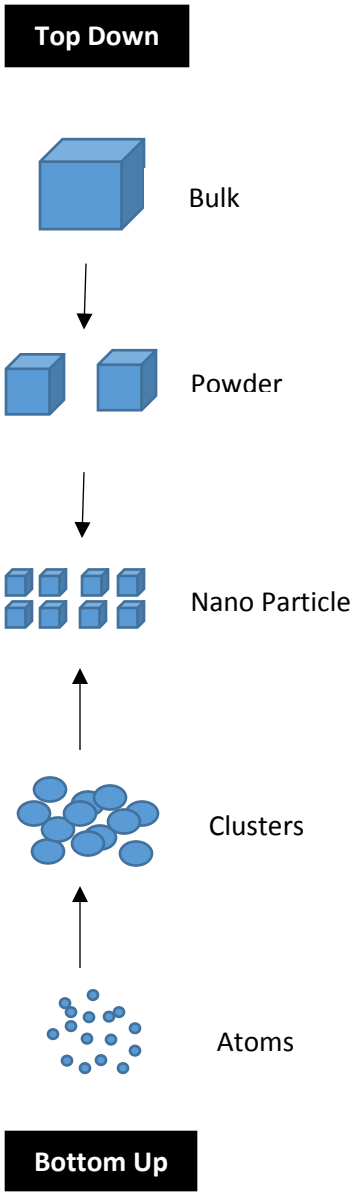

Figure. 1.1: Flow chart of top-down and bottom-up approach of the building up of Nanostructure.

1.2 Applications of Nanomaterials:

Nanomaterials have lots of applications in diverse fields, some of them are as follows:

i. Nano materials are used in cancer imaging and therapy [1].
ii. Nano materials have applications in Bio-sensors and Bio-medicine [2, 3].
iii. Nano materials are used in water disinfection and bio-control [4].
iv. Nano ferrites are used in electronic, electrical and magnetic devices [5].
v. Nano ferrites are used for power applications [6].
vi. Nano ferrites are used for high frequency applications [7].
vii. Nano ferrites are also used as nano-catalysts [8].
viii. Nano ferrites are widely used in cosmetics, textile, agriculture and product of sports etc.

1.3 Magnetic Materials:

All materials are divided into two main types:

i. Non-Magnetic Materials:

Materials in which no magnetic domains are present. For example: wood, glass and plastic etc.

ii. Magnetic Materials:

Materials in which magnetic domains exist such as steel, iron, copper etc. magnetic materials are not extensively existing materials but have great importance in advance fields and conventional fields. There are two main types of magnetic materials, discussed as follows:

1.3.1 Soft Magnetic Materials:

Materials which can retain their magnetism for short period of time and by applying external magnetic field, they are easily magnetized such as iron

[9].They are having applications such as small electronic transformers stators, cores of power transformers and rotor materials for generators and motors. [10]

1.3.2 Hard Magnetic Materials:

Materials which can retain their magnetism for considerable long time and by applying external magnetic field,they are not easily magnetized as steel. Hard magnetic materials are also named as permanent magnets. They are having applications such as in telephone receivers, loud speakers and automotive starting motors.[11]

1.4 Classification of Magnetic Materials:

As we apply the magnetic field. Materials can behave in a different way in response, due to various reasons like atomic or molecular level of structure, magnetic moments of atoms. As each electron has magnetic moment, the value expressed as Bohr magnetron is 9.27× 10 -24 Am2. An electron has got magnetic field due to spin around its own axis and orbital motion about nucleus, both movements are affected by applied magnetic field. In atoms, electrons usually pair up with opposite spins, cancelling net magnetic field. So, magnetic field is present only in those atoms, ions which have odd no. of electrons. For example: iron, trivalent iron has a moment equal to 5 un cancelled spins.

Based on these behaviors, materials can be classified in different categories:

1. Diamagnetic materials.
2. Paramagnetic materials.
3. Ferro/Ferrimagnetic materials.
4. Antiferromagnetic materials.
5. Superparamagnetic materials.

These categories are explained as follows:

1.4.1 Diamagnetic Materials:

The materials in which even no. of electrons are present due to which spins are balanced and net magnetic moment gets zero. Magnetic field generated due to orbital motion is opposite to applied field, due to which these materials show negative magnetic susceptibility as shown in Fig. 1.2. For example: gold, bismuth, copper, wood and plastic etc.

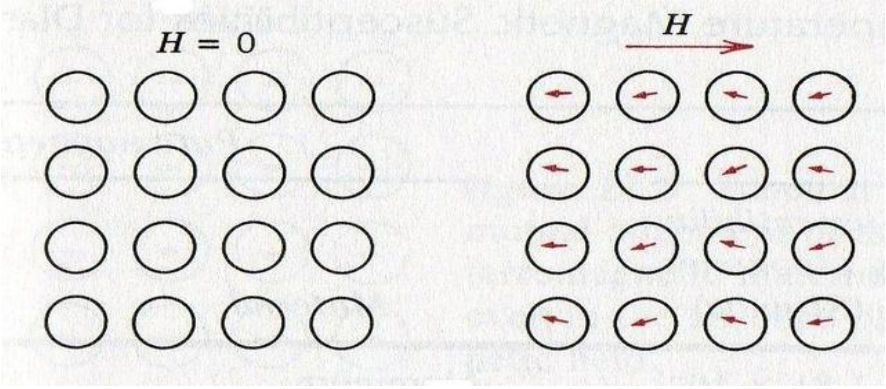

Fig. 1.2: A diamagnetic material [12].

1.4.2 Paramagnetic materials:

In these materials some spins due to orbital motion and spinning remains unbalanced, this incomplete cancellation of spins results in atoms behaving as tiny magnets, these small magnets do align on application of external magnetic field and are called as paramagnetic materials as shown in Fig. 1.3. Such materials show slight attraction towards magnets, proving low positive magnetic susceptibility. For example: Tungsten, cesium and sodium etc.

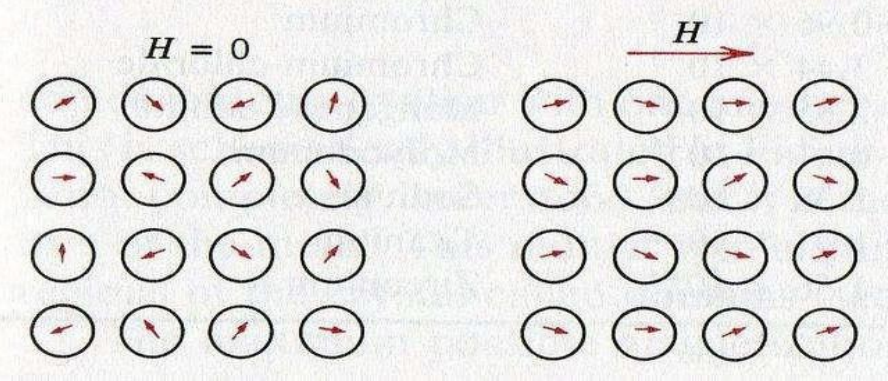

Fig. 1.3: a Paramagnetic material [12].

1.4.3 Ferromagnetic Materials:

These materials show great affinity towards magnetic field even when the applied magnetic field is removed as maximum number of domains remained aligned even after removal of magnetic field due to the presence of unpaired electrons and eventually of having overall net magnetic moment. These materials have positive magnetic susceptibility as shown in Fig. 1.4. For example: iron, nickel, cobalt, ferrites and magnet garnets etc.

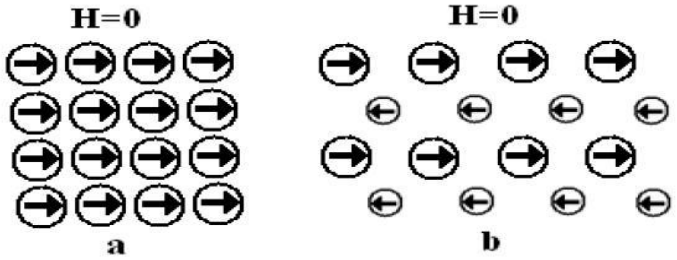

Fig. 1.4 Ferromagnetic and Ferrimagnetic material [12].

1.4.4 Ferrimagnetic materials:

These materials have complex crystal structure as of ionic compounds. These materials are similar to ferromagnetic materials but in presence of

applied external magnetic field few dipoles align opposite to the direction of magnetic field and few align parallel to the magnetic field but their amount is not equal due to which complete cancellation do not occur and net magnetic moment less than ferromagnetic materials is observed as shown in Fig. 1.4. For example: ionic compounds and oxides.

1.4.5 Anti-Ferromagnetic materials:

In these materials, the magnetic moments are directly related to the spin of electrons and with the spin of neighboring electrons oriented in opposite direction. So, cancellation of magnetic moment takes place but magnetization is having small positive value. The behavior of anti-ferromagnetic materials as shown in Fig. 1.5 is seen at lower temperatures but above a specific temperature known as Neel Temperature these materials behave as paramagnetic materials. [13] For example: chromium, nickel oxide and iron manganese alloys etc.

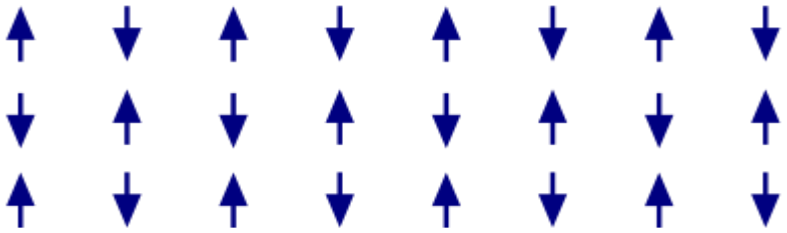

Fig. 1.5 Anti-ferromagnetic materials [12].

1.4.6 Superparamagnetic materials:

These materials as shown in Fig. 1.6 behave like paramagnetic materials below curie or Neel temperature (The temperature at which ferromagnetic or ferromagnetic starts acting like paramagnetic that is lose their magnetic property). In these materials, large internal magnetic fields are created by the alignment of magnetic moments of neighboring atoms caused due to the action of coupling forces.[14]

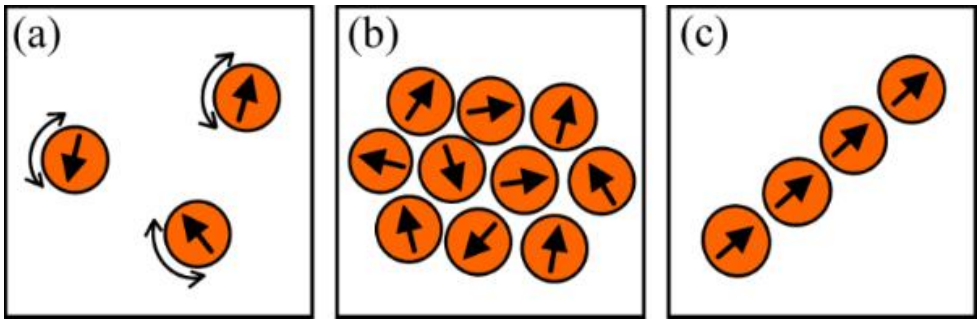

Fig. 1.6 Superparamagnetic ordering of dipoles [12].

1.5 Ferrites:

Ferrites are one of the most important ferrimagnetic materials that is they can be attracted towards magnet, mainly composed of iron oxide and are electrically insulators. Magnetite is the natural ferrous ferrite represented as Fe (Fe_2O_4) or Fe_2O_3. Cores of transformer and permanent magnets are made by magnetic materials like ferrites. The electrical resistivity of ferrites is really high due to which they are mostly used in high frequency applications. On the basis of mass and charge of metallic ion, ferrites can be classified into two structural symmetries that are cubical and hexagonal. Two types of ferrites based upon hysteresis loss are as follows:

1.5.1 Soft Ferrites:

Ferrites having low magnitude of coercivity are known as soft ferrites. They have high resistivity, low magnetostriction, low remanence and low permeability. They take less time to magnetize or demagnetize, therefore less energy loss during magnetization, due to which are used to reduce and prevent energy losses in inductors and transformers. They are brittle, hard and are gray or black in colour. For example: Mangnese-Zinc ferrite, Nickle-Zinc ferrite.

1.5.2 Hard Ferrites:

Ferrites having high magnitude of coercivity are known as hard ferrites. They have low resistivity, high magnetostriction, high remanence and high permeability. These ferrites take more time to magnetize or demagnetize,therefore more energy loss during magnetization. These materials are easily available and cheap as they are made from cheap materials like strontium, iron and barium oxides. They are commonly called as ceramic magnets, are used in household appliances. For example: Cobalt ferrite and Strontium ferrite.

1.6 Types of Ferrites:

According to the type of structure, ferrites can be classified into three catogeries:

1. Spinel ferrites.
2. Garnet ferrites.
3. Hexagonal ferrites.

1.6.1 Spinel ferrites:

Spinel ferrite is a soft ferrite having general formula as MFe_2O_4 , where M is general representation of divalent metal ion. For example: Nickel (Ni^{+2}), Copper (Cu^{+2}), Zinc (Zn^{+2}), Cobalt (Co^{+2}), Iron (Fe^{+2}). 32 oxygen atoms, 8 divalent metal cations and 16 trivalent iron ions are present per unit cell of spinel ferrite. Two types of interstitial sites are present between anions named as A (tetrahedral sites) and B (octahedral sites) sites as shown in Fig. 1.7, which are occupied by metal ions.

1.6.1.1 Tetrahedral sites:

The sites which are surrounded by 4 oxygen atoms, total number of tetrahedral sites in spinel ferrites is 64, out of which, 8 tetrahedral sites are occupied by cations like Cu^{+2},Co^{+2}, Ni^{+2} etc.

1.6.1.2 Octahedral sites:

The sites which are surrounded by 6 oxygen atoms, total number of octahedral sites in spinel ferrites is 32,out of which,16 octahedral sites are occupied by anions.

Electrically neutral spinal structure is formed after filling of all tetrahedral and octahedral sites.

Table 1.1 Radii of some common metal ions used in the spinel ferrites [15].

Ion	Ionic radius Å
Fe^{2+}	0.83
Fe^{3+}	0.67
Co^{2+}	0.82
Zn^{2+}	0.74
Ni^{2+}	0.78
Mn^{3+}	0.70

1.6.1.3 Types of Spinel ferrites:

Two types of spinel ferrites are classified on the structural basis, are described as follows:

a. Normal Spinel ferrite:

In normal spinel ferrites, all tetrahedral sites are occupied by divalent metal ions and all octahedral sites are occupied by trivalent metal ions. For example: Cadmium ferrite, Zinc ferrite etc.

b. Inverse Spinel ferrite:

In inverse spinel ferrites, tetrahedral sites and octahedral sites both are occupied by trivalent metal ions and all divalent metal ions occupy just octahedral sites. [15] For example: Nickel ferrite, Copper ferrite, Mangnese ferrite etc.

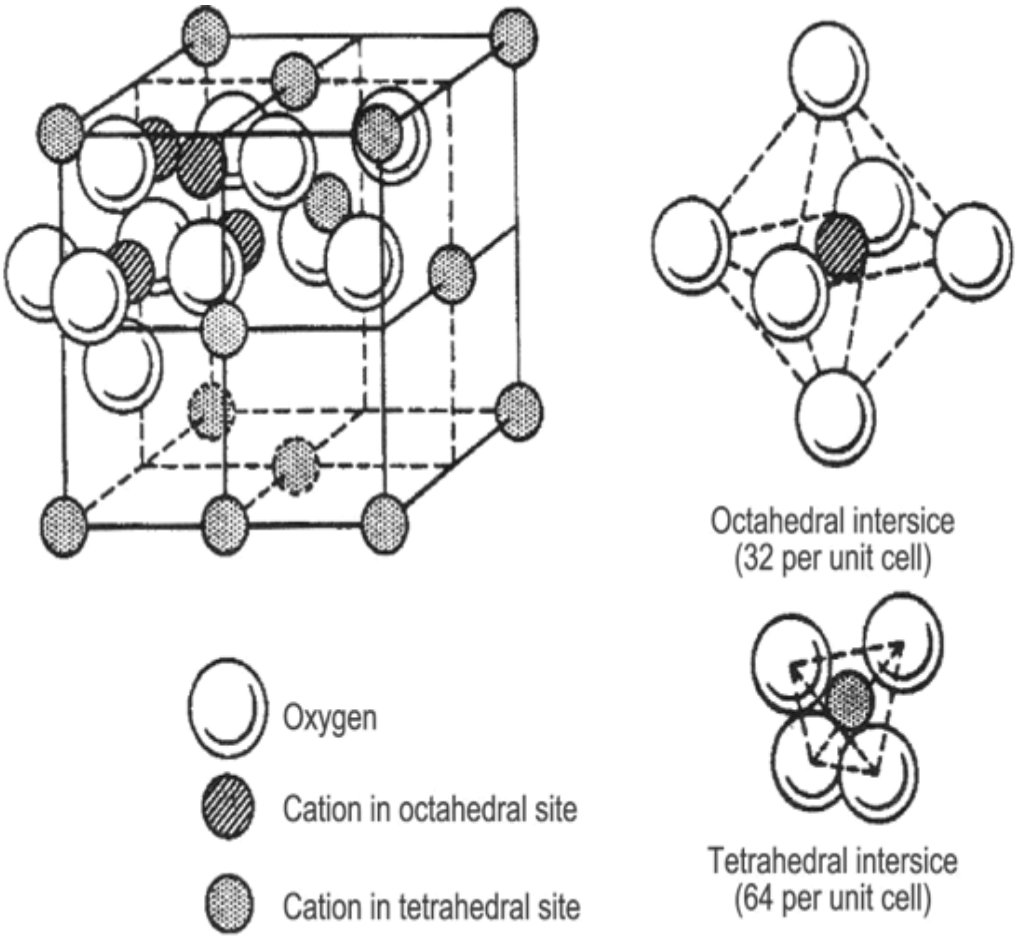

Fig 1.7: Spinel ferrite unit cell with octahedral and tetrahedral sites [12].

1.6.2 Garnet ferrites:

Galileo and Griller discovered a new type of ferrite named garnet ferrites in 1957. The general formula of these ferrites is $M_3Fe_5O_{12}$. In this formula M represents

the rare earth trivalent ions like Y, Gd, and Dy. Nature wise these ferrites are cubic and hard magnetic materials.

1.6.3 Hexagonal ferrites:

The general formula of hexagonal ferrites is $MFe_{12}O_{19}$. In this formula M is barium, cobalt, strontium or it can be any other combination. These ferrites are same as spinel ferrites as can be used as hard magnetic materials and have cubic structure but the difference is in the number of interstitial sites, hexagonal ferrites have three sites namely octahedral, tetrahedral and trigonal. They are used in many different applications. For example: microwave ovens, permanent magnets and magnetic recording devices etc.

Table 1.2 : An Overview of different types of ferrites [16].

Type	Structure	General Formula	Example
Spinel	**Cubic**	**$M^{II}Fe_2O_4$**	**M^{II}=Fe,Cd,Co,Mg,Ni and Zn**
Garnet	**Cubic**	**$M^{III}{}_3Fe_2O_{12}$**	**M^{III}=Y,Sm,Eu,Gd,Tb and Lu**
Magnetoplumbite	**Hexagonal**	**$M^{II}Fe_{12}O_{19}$**	**M^{II}=Ba,Sr**

1.7 Nickel ferrite:

Nickel ferrite is an inverse spinel in which half of ferric ions occupies the octahedral sites (B-sites) and other half occupies the tetrahedral sites (A-sites) ,compound can be represented as $(Fe^{3+}_{1.0})_A$ $[Ni^{2+}_{1.0}Fe^{3+}_{1.0}]_B$ 0^{2-}_4 [17, 18]. The excellent magnetic and electrical properties of nickel ferrite depends on factors like charge, nature of metal ions and their distribution.[19]

Nickel ferrite is a soft ferrite widely studied owing to its different properties like good electromagnetic performance ,normal saturation magnetization and high electrical resistivity [20]. It's importance is highly increased due to its large number of applications such as gas sensor [21], thin films [22], Ferro fluids [23],catalysts [24] ,magnetic materials and microwave absorbing equipment. [18, 19, 25-29]. Several methods have been devised for synthesis of NiFe2O4 such as hydrothermal synthesis,[30] sol-gel auto combustion,[19] [31] thermal decomposition, [32] thermolysis, [33] co-precipitation, [34] gel-assisted hydrothermal, [35] microwave synthesis [36] and wet chemical co-precipitation techniques.[37]

High weight with low dielectric loss puts limits to its use as microwave absorption material [38] so, to solve this problem, dielectric lossy materials are added like carbon nanotube, carbon nanoparticle, carbon nanofiber and graphene etc. [39-41]

1.8 Applications of ferrites:

Nanoparticles of ferrites have lots of applications due to below described properties:

a. Mechanical stability.
b. Electrical stability.
c. Temperature robustness.
d. Time stability.
e. Cheap.
f. Easily available raw materials.
g. Good dielectric properties.
h. High frequency applications.
i. Microwave frequencies applications.

j. Varied and wide range of materials.
k. High value of coercivity of some ferrites.
l. Good magnetic properties.

Nano ferrites are used in electronic, electrical and magnetic devices. [5], are used for power applications. [6], high frequency applications. [7], are also used as nano-catalysts. [8], in cancer imaging and therapy. [1], in Bio-sensors and Bio-medicine. [2, 3], in water disinfection and bio-control. [4]

1.9 Introduction to Carbon Nanofibers:

Cylindrical nanostructures of graphene layers arranged as stacked plates, cups or cones over each other are called as Carbon nanofibers. If these Carbon nanofibers are wrapped into cylinders, Carbon nanotubes are formed.

Carbon has lots of versatile compounds whether organic or inorganic due to its unique ability of existing in sp, sp^2 and sp^3 hybridizations. Carbon has the ability to form unique structures, filaments or fibers known as Carbon nanofibers. Carbon nanofibers are short carbon fibers, which have got particular attention due to its wide range of applications in frequency shielding, electrical, thermal and mechanical properties enhancements [42].

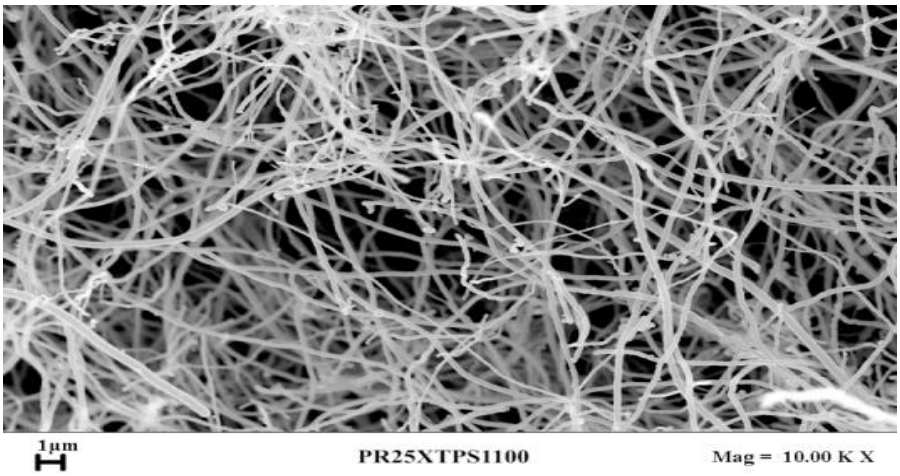

Fig. 1.8 Carbon nanofibers

(Adapted from: Wikipedia)

Carbon nanofibers were first synthesized in 1889 by Hughes and Chambers. They used mixture of hydrogen and methane gases, grew fiber by the help of gas pyrolysis and carbon deposition.[43] Radushkevich and Lukyanovich in 1950 observed carbon nanofibers for the first time with the help of electron microscope, [44] then Morinobu Endo in 1970 also announced discovery of carbon nanofibers including hollow tube like fibers [45]. In 1980 Tibbetts in the USA modified the fabrication process of Carbon nanofibers [42, 46].

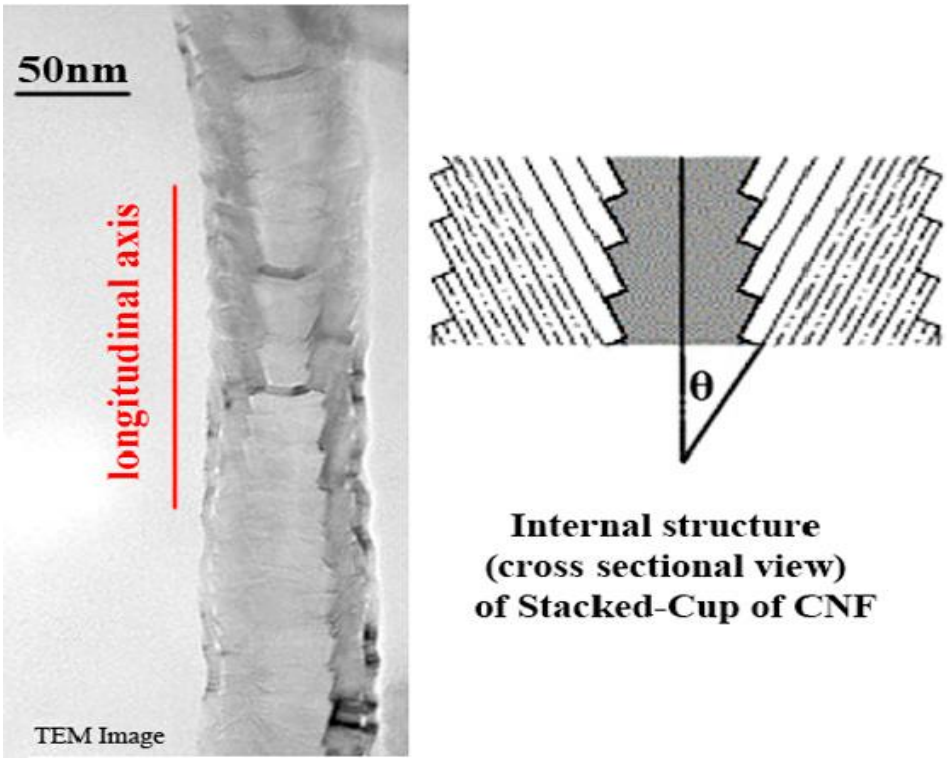

Fig. 1. 9 cross sectional view of CNF [47].

1.9.1 Applications:

Due to their exceptionally good properties, easy availability and cheapness, Carbon nanofibers are extensively used as follows:

a. In field electron emission sources.
b. Carrier material for catalysts petrochemistry.
c. In gene delivery as vertically aligned arrays.

d. Oil spill remediation.
e. For electrode materials [48].
f. In making composites for enhancement of the properties of original components etc.

1.9.2 Advantages of using CNF's:

There are several benefits of the use of CNF in comparison to CNT's, described as follows:

a. They can easily be dispersed.
b. They can provide mechanical and electrical enhancement equally well.
c. They are easier to process.
d. They are easier to functionalize.
e. They are not only cheap themselves, but also reduce the cost of overall process.

1.10 Nanohybrid of $NiFe_2O_4$ / CNF:

Nanoscience is the most growing research field. This highly growing field is used for synthesizing new materials of great potentials .Ever growing energy needs are compelling and motivating the scientists to research about synthesis of new potential energy storage sources.

Due to great physical and electrical properties of carbon nanomaterials such as carbon nanotube and carbon nanofiber, they have attracted lots of attention in research these days. Carbon nanofiber has attracted more attention due to its easy availability, cheapness, chemical purity, physical strength, chemical inertness and great electrical properties.[39, 49].

Now a days, researchers are trying to combine two or more materials having complementary properties to synthesize a hybrid having enhanced properties of both the component materials. Spinal ferrites have general formula MFe_2O_4 ,(M= Ni ,Zn ,Mn, Co and Mg) [18] $NiFe_2O_4$ nanoparticles are widely studied magnetic oxides due to their good electrical, optical and magnetic properties. [50] Their marvelous properties like high permeability ,high electrical resistivity, and least values of eddy current losses for high frequency electro-magnetic wave propagation proves

them appropriate for lots of technical applications as gas sensors ,magnetic storage, magnetically guided drug delivery, microwave absorption devices, in telecommunication and magnetic fluids. Several methods have been devised for synthesis of $NiFe_2O_4$ such as hydrothermal synthesis,[30] sol-gel auto combustion,[19] [31] thermal decomposition, [32] thermolysis, [33] co-precipitation, [34] gel-assisted hydrothermal, [35] microwave synthesis [36] and wet chemical co-precipitation techniques.[37] The properties of Nano ferrites largely depends on particle size. Due to large surface areas of nanoparticles, there properties are enhanced as compared to bulk materials.

Nanocomposite of ferritic matrix and Carbon nanofiber as filler are having advantage that their properties such as optical ,magnetic ,dielectric, microwave absorbance and electrical can be optimized as per requirement by changing the percentage of Carbon nanofiber in the composite, which renders them useful for many new applications, such as electrode material for batteries, electrical devices, sensors and supercapacitors [51, 52] Carbon nanofiber shows more potential of storing energy [53].

Now a days, energy demands are increasing manifolds, such that it is becoming difficult to meet the energy needs day by day. Due to increased burning of fossil fuels, environmental problems are increasing gradually and the reserves of fossil fuel are also depleting. So, it is the need of hour to think and focus towards other sources of energy and efficient energy storage devices are required to be fabricated. To fulfill our this need,we should focus towards the enhancement of dielectric properties.

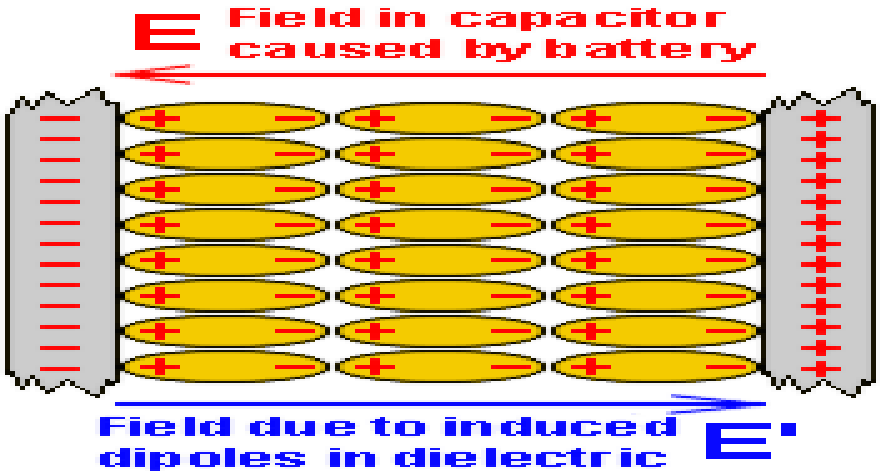

Fig. 1.10: The dielectric dipole orientation in the capacitor [54].

In order to enhance the dielectric properties, let's suppose two neutral conducting metal plates, which are separated by distance'd', if a battery of certain potential is connected to both of these plates, the cathode of the battery will induce positive charge on the plate adjacent to it and the anode of the battery will induce negative charge to the plate in connection with it. As no conducting material is present between plates, charges cannot flow, as a result potential is created between plates, now, even if we remove the battery, charges stored on plates will creat the ability of doing work for any device. The non-conducting or insulating material present between plates is referred as dielectric material, this dielectric material is performing two major duties for us. Firstly in a way that it is maintain a distance between plates helping to creat potential, secondly it is creating the additional potential, stored working power for the system by allowing the electric field generated by the potential between plates to align it's dipoles along the lines of the force of the field, thus allowing the capacitor to store more charge and as a result more energy to do the work as shown in Fig. 1.10.

In our presented work, the Carbon nanofibers will act as the high surface area plates, thus with the ability to store more charge and nickel ferrite nanoparticles will act as dielectric medium between the Carbon nanofibers. The ability to store charge can be increased by increasing the dipole moment or surface area of plates..In our work, the nickel ferrite nanoparticles were prepared by employing wet chemical co-precipitation route. Ortho-xylene was used as a solvent to disperse the commercially available Carbon nanofibers and synthesized nickel ferrite nanoparticles uniformly, after which manual grinding was done to completely homogenize both components. The formation of the nanohybrid was confirmed and studied using XRD and SEM. The electrical properties were studied by impedance analyzer.

In this research, we introduced a novel, facile and one step method of synthesizing $NiFe_2O_4$/CNF (CNF= 10%, 15% and 20%) nanohybrid and have tried to study its physical, structural, dielectric and impedance properties, which rendered this material useful for high frequency applications, supercapacitors and microwave devices.

1.11 Objectives:

The objectives of our research work are as follows:

a. To synthesize nickel ferrite nanoparticles by inexpensive and very simple wet chemical co-precipitation method.
b. To synthesize nanohybrid by a one-step facile method using ortho-xylene as dispersive medium.
c. To study the effect of increasing concentration of Carbon nanofibers on the electrical properties of $NiFe_2O_4$ / CNF nanohybrid.

Chapter 2

Theoretical Review

2.1 Synthetic Approaches for Nanoparticles:

There are two main synthetic approaches for nanoparticles synthesis:

- Top down approach.
- Bottom up approach.

  When we synthesize nanoparticles by breaking larger particles to nanoparticles, this approach is known as top down approach. For example: lithography, etching, and mechanical attrition.

  When we build up nanoparticles from atomic scale, this approach is known as bottom up approach. For example: chemical synthesis, aerosol compaction.

2.2 Synthesis Techniques of Nanoparticles:

Various techniques are available for synthesis of nanoparticles, every technique has its own prose and corns, every technique gives different structural, magnetic and electrical properties. Some of the techniques or methods are mentioned as follows:

- Sol-gel technique.
- PolyVinyl Alcohol (PVA) Evaporation technique.
- Gas condensation process.
- Combustion Flame Synthesis.
- Micro Emulsion Method.
- Chemical Co-precipitation Method.
- Sono Chemical Method.
- Hydro-Thermal Method
- Solvo-Thermal Method

In sol-gel technique, complete homogeneity is obtained. It has an advantage that it is a cheap technique as well as can control product formation at low temperatures, has got many applications in electronics and optics.

As PVA is a cheap and easily available solvent, so, this method has an advantage of cheap and uniformly sized formation of nanoparticles.

Gas condensation process uses inert gas at high pressure enough to allow the formation of nanoparticles in vacuum chamber but in this method, it is difficult to achieve the formation of spherical particles.

Flame processes were introduced for large scale or commercial scale manufacturing of nanoparticles. The popularity of this method was due to its one step process and no moving parts machinery, however it is having a drawback that the product characteristics cannot be controlled completely [55].

In micro emulsion technique, some surfactant is dissolved in organic solvent forming revere micelle, the water molecule is surrounded by surfactant molecules and forms a water pool, which acts as micro reactor for the formation of nanoparticles, precipitation is used for the formation of fine ferrite nanoparticles formation in these water in oil micro reactors [56].

In Sono Chemical method, reactants or the starting materials are reacted under ultrasonic waves, this method achieves reduction of size, uniformity of dissolution and morphological control [57].

Hydro-thermal /solvo-thermal method is low-cost,easy method,achieves very good control on morphology of nanoparticles. Different crystals like nanosphere, nanorods, nanocrystal, hollow sphere,urchin like crystals and nano-rod bunches can be formed with the help of this simple process just by controlling re-crystallization.

In our present work, we made nanoparticles by Co-Precipitation technique, so, only this method is discussed in detail as follows:

2.3 Chemical Co-precipitation Method:

This is very easy method which utilizes very short time for the synthesis, however having disadvantages of the production of fumes and inability to control the particle size precisely is also there. In this process, reactants are dissolved in water in predetermined ratios with the addition of sodium hydroxide to maintain the pH. When precipitation starts, nucleation occurs but quickly forms thermodynamically more stable growths, for the phenomenon of co-precipitation to occur, rate of nucleation should be greater than the rate of growth.

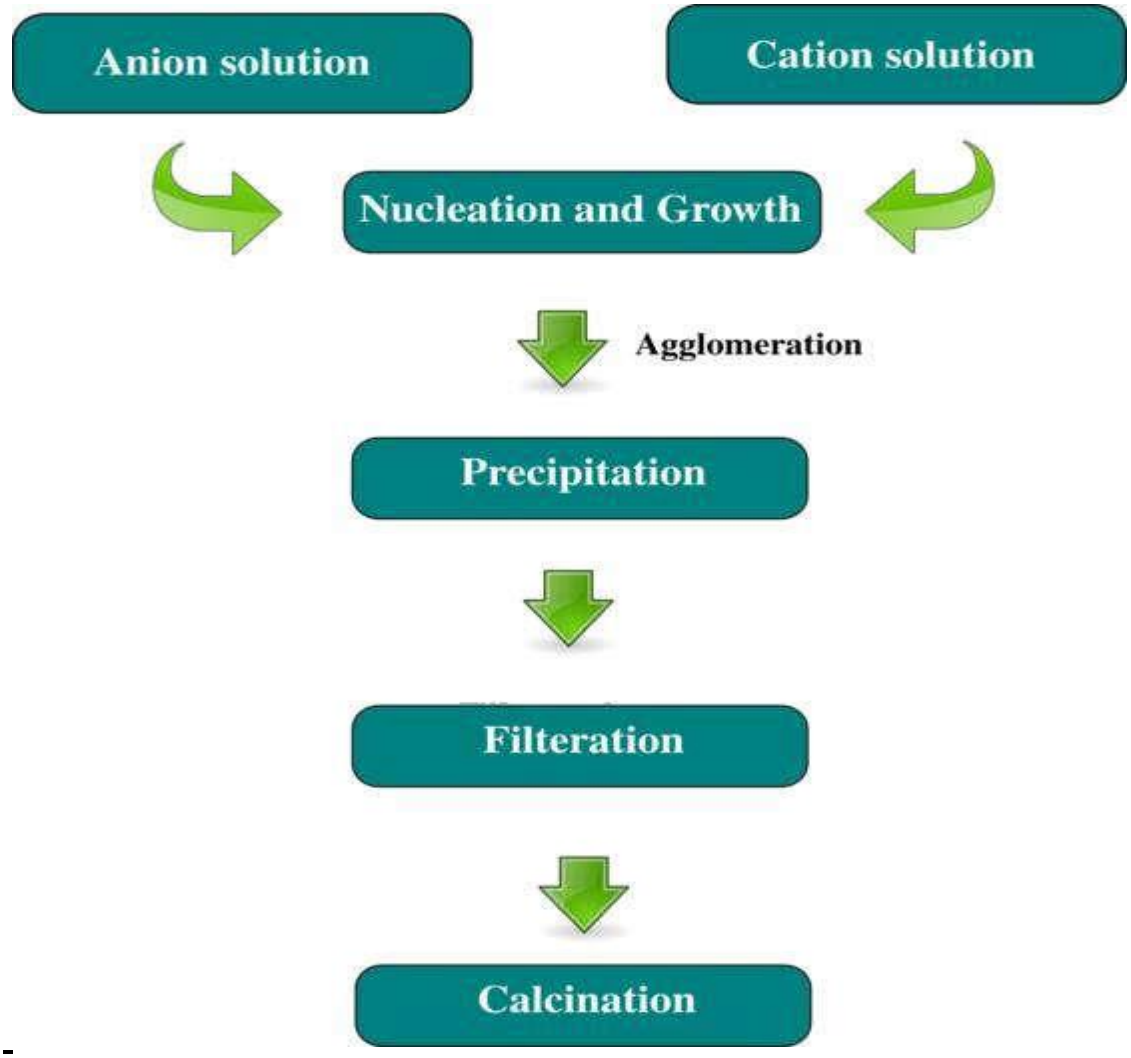

Fig. 2.1 Steps for the process of Chemical Co-precipitation

There are two main ways for the production of oxides, some oxides are synthesized directly while in other method, the precursor formed requires drying and calcination to be done afterwards. Settling down of precipitates at the base of beaker occurs in process of co-precipitation, then filtration is done, after that they are washed with water several times to remove all the impurities present in the sample, then they are air dried.

Co-precipitation is an easy and good method as it is low cost, cheap and great method, which enables the formation of cheap and homogeneous nanoparticles.

The crystallinity of the nanoparticles is affected by the rate of reaction and impurities. Nucleation, growth rate, super saturation affects the shape and size of nanoparticles. When super saturation is high, reduction in the size of particles is experienced. Rate of reaction and transport of chemicals is affected by the concentration of reactants. Precipitation is affected by no. of factors including temperature and pH. Usually sodium hydroxide is used for precipitation [58].

2.3.1 Main steps in Co-precipitation:

The two main steps are as follows:

a) Co-precipitation step.
b) Ferritisation step.

2.3.1.1 Co-precipitation step:

In this step, solid metallic hydroxides are obtained in iron nitrate and sodium hydroxide solution by the co-precipitation. In our case that is for nickel nitrate, reaction is as follows:

$$Ni\,(NO_3)_2.\ 6H_2O\ +\ Fe\,(NO_3)_3.\ 9H_2O + NaOH$$

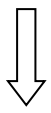

$$Ni\,(OH)_2.\ Fe\,(OH)_3 +\ NaNO_3$$

2.3.1.2 Ferritisation step:

In this step above mentioned metallic hydroxide solution is further heated to convert it to ferrite of nickel. The reaction is as follows:

$$Ni(OH)_2 . Fe(OH)_3 + NaNO_3$$

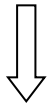

$$NiFe_2O_4 . nH_2O + (4-n)\ H_2O + NaNO_3$$

Size, shape and precipitation of nanoparticles depends upon no. of variable factors. All the impurities mainly that are ionic in nature are removed by washing multiple times with de-ionized water until pH turns to 7 or neutral.

2.3.2 Factors upon which Co-precipitation depends:

The factors which affect the process of co-precipitation are mentioned below:

- Effect of pH.
- Effect of temperature.
- Mixing rate of the reagents.
- Role of cations.
- Heating after co-precipitation.

The above mentioned factors are described as follows:

2.3.2.1 Effect of pH:

pH affects vitally in controlling the size and shape of nano ferrites. There is no significant growth rate at low pH values. So, at low pH values growth rate is low and at high.

pH values, growth rate is high. In our case of nickel ferrite the pH range is 11-12. As the growth rate is high at high pH values, so, the time required for the formation of the product is decreased.

2.3.2.2 Effect of temperature:

There is rapid formation of nano ferrites normally from 20^{o} -70^{o} C. Different metals have got different values of activation energies for the formation of nano ferrites even at same temperature. When we heat the reactant containing solution, activation energy is provided. In our case for nickel ferrite, the range of temperature is 70^{o} - 100^{o} C.

2.3.2.3 Mixing rate of the reagents:

Size of nanoparticles is highly affected by the mixing rate of the reagents. Two processes of nucleation and growth are very important in determination of the size of nanoparticles. Small size particles are formed, if nucleation rate is high and growth rate is low while large size particles are formed, if growth rate is high and nucleation rate is low. Nucleation rate should be higher than the growth in order to achieve good mixing of reagents. So that, small and homogeneous nanoparticles can be obtained. The rate of mixing is high, if nucleation rate is higher than growth rate and viceversa [59].

2.3.2.4 Role of cations:

Different metals have different properties, their different properties also affect the properties of nano ferrites. Thus the nature of cation or metal has a great influence on properties of ferrites. To achieve better results metal salts should be used. Mostly metal salts of sulphates, nitrates and chlorides are used.

2.3.2.5 Heating after co-precipitation:

At the end of process of co-precipitation, for distinct phase formation, annealing is required. For the attainment of small size and distinct phase, both the amount and duration of heating are equally and extremely important.

2.3.2.6 Advantages of Co-precipitation method:

There are several benefits of Co-precipitation method over other synthetic methods:

a) This is a simple method.
b) This method requires less time.
c) Particle composition can be controlled.
d) Size and shape of nanoparticles can also be controlled.
e) Homogeneous nanoparticles which are small in size can be obtained by utilizing this method.

2.4 Synthesis of Nickel ferrite:

Nickel nanoferrite particles were prepared by wet chemical co-precipitation route. Nickel (II) nitrate hexahydrate (Ni $(NO_3)_2.6H_2O$) provided by ACROS ORGANICS, New Jersey USA 1-800-ACROS-01 Geel, Belgium (99% purity), Iron (II) nitrate nonahydrate (Fe $(NO_3)_3.9H_20$) provided by EMSURE® Merck KGaA Darmstadt Germany (99% purity), Sodium hydroxide provided by Fischer Chemical Ltd. Hong Kong and CNFs provided by Sigma Aldrich were used. All these reagents were of analytical grade and used as received without any further purification.

Double distilled deionized water was used to prepare 300ml solution of 0.1M Nickel (II) nitrate hexahydrate (Ni $(NO_3)_2 \cdot 6H_2O$) and 300 ml solution of 0.2 M iron (III) nitrate Nona hydrate ($Fe(NO_3)_3.9H_20$) and these above two solutions were mixed with each other, followed by constant stirring for about 20 min at room temperature. The entrance of impurities in the obtained product was prevented by the usage of double distilled deionized water. Along with constant stirring, this mixture of solutions was then heated to 90 °C and 300 ml solution of a 3 M sodium hydroxide (NaOH) was heated to 90 °C separately and then added in the above mixture. The pH of the solution was ensured to be at 12. The solution was washed with double distilled deionized water several times till pH was neutralized to 7, to attain impurity free Nickel ferrite nanoparticles as a precipitate along with small amount of water contents which were evaporated by heating it overnight at 100 °C in the oven and dried powder of nickel ferrite nanoparticles was obtained. A

well distinct spinal phase was obtained by calcinating the powder for 6 hours at 800 °C using muffle furnace and carbonaceous impurities were removed as a result. Manual grinding of the product was done and was characterized by different techniques i.e. Scanning Electron Microscope, X-Ray Diffraction, Impedance Analyzer and Fourier Transform Infrared Spectroscopy.

Pellets were made for checking dielectric properties using hydraulic press, 4 tons pressure was applied for 3 minutes duration. Pellets were further sintered at 500 °C for 2-3 hours.

2.5 Xylene as a solvent /dispersive medium:

The word xylene is derived from greek word "xylo" meaning wood because this also smells like wood. Xylene is also named as xylol or dimethyl benzene. It is an aromatic compound with the formula $(CH_3)_2C_6H_4$ having three isomers, each having benzene as central ring substituted by two methyl groups whether at 1, 2 positions named as ortho-xylene, at 1, 3 positions named as meta-xylene or at 1, 4 positions named as para-xylene. All three isomers are colorless, flammable liquids as shown in Fig. 2.2.

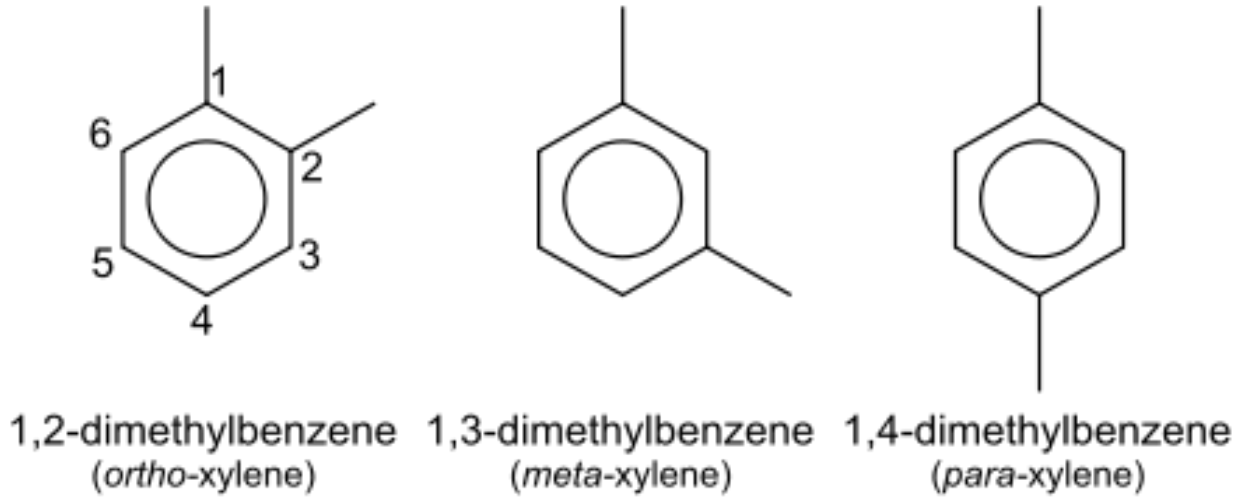

Fig. 2.2 Isomers of Xylene [60]

Xylene is often used as solvent owing to its following properties:

- The density of ortho-xylene is 0.88 g/mL and that of meta-xylene, para-xylene is 0.86 g/mL and so, the density of xylenes is 0.864 g/mL, which is even lower than water. This property of having lower density than water renders it useful as good dispersive medium.
- As benzene is an aromatic compound, its ring is electrophilic in nature and electrons are shared between all six carbons, other bond electrons are also attracted by benzene ring, in the same way nickel and iron has tendency to lose electrons towards benzene ring of xylene, forming Ni^{+2} and Fe^{+2}, Fe^{+3} respectively. Thus this benzene ring of xylene enables to act as good dispersive medium for ferrites and weak Vander walls attractions or weak polarizations also helps it to be good dispersive agent for CNFs and nickel ferrites nanoparticles.

2.6 Synthesis of $NiFe_2O_4$/CNF Nanohybrid:

To prepare Nickel ferrite/CNF Nano hybrid, pre-obtained CNFs and synthesized nanoparticles of Nickel ferrite annealed at 800 °C were separately taken in two 250 ml beakers each containing 100 ml of Ortho-xylene and were uniformly dispersed with the help of ultrasonicator, sonication was done for several hours (12-14) at room temperature. The uniformly dispersed ferrite particles in Ortho-xylene medium were then drop wise added to CNFs dispersion and the resulting mixture was again sonicated for 12 h using water bath ultra sonicator. The residual Ortho-xylene solvent was evaporated, which left behind uniformly dispersed Nano hybrid and mechanical mixing was done to further homogenize the nanohybrid. Effect of increasing CNFs concentration was studied by changing the weight percentage of CNFs (10%, 15%, and 20%). Different properties of the prepared Nano hybrid were evaluated. The material under investigation was finely ground manually, homogenization was done and average bulk composition was determined. In the presented work, Stoe Diffractometer system with CuKα radiation (1.5405 Å) was used to study about phase and crystal system of the prepared nanoparticles and Nano hybrid at room temperature. Perklin Elmer Spectrum was used to carry out Fourier Transform Infrared Spectral (FTIR) analysis, the presence of metal-oxygen vibrations was confirmed using FTIR spectrometer in $NiFe_2O_4$ nanoparticles and Nano hybrid. JEOL JSM-6390 scanning electron microscopy (SEM) was used to evaluate microstructures of the prepared

samples. Wayne Kerr LCR 6500B was used to investigate in detail the dielectric properties. The dielectric parameters are calculated by using relations [61].

2.7 Summary of Experimentation:

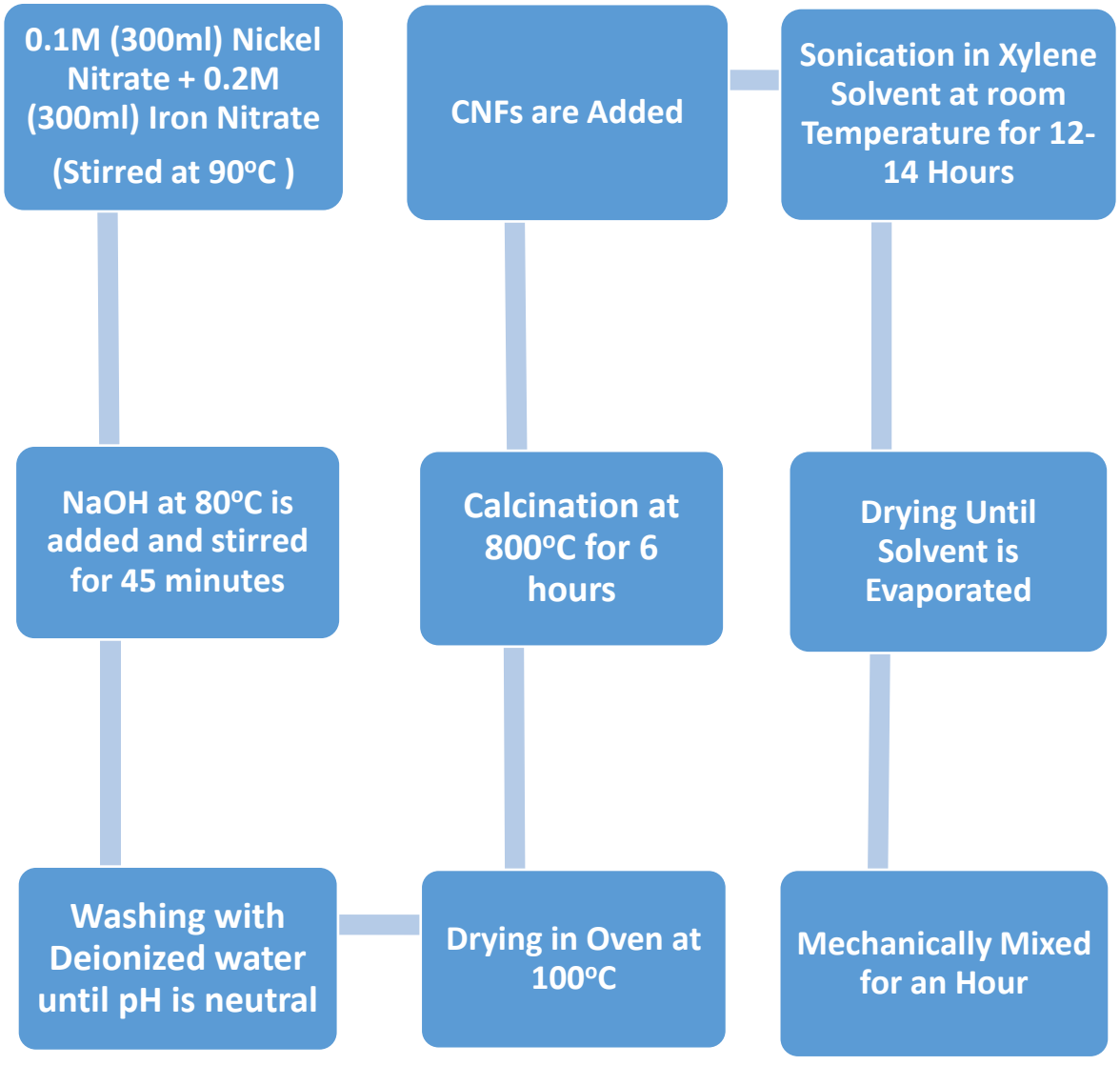

Fig. 2.3: Summary of the experimentation

Chapter 3:

Introduction to Sample Characterization Techniques.

3.1 Introduction:

To study the usage or importance of any material, it is essential to evaluate its properties, for this purpose, different characterization techniques are utilized.in our case to study the properties of nickel ferrite and its coating on carbon nanofibers, these following characterization techniques are utilized:

a) X-Ray Diffraction Technique

- ❖ Particle Size and Lattice parameter determination
- ❖ Mass Density and X-ray Density calculations
- ❖ Phase formation
- ❖ Porosity Calculations

b) Fourier Transformed Infrared Spectroscopy

c) Scanning Electron Microscope

- ❖ Structural observations
- ❖ Surface morphology

d) Impedance Analyzer

- ❖ AC Conductivity
- ❖ AC Impedance Spectroscopy
- ❖ Dielectric properties.

3.2 X-Ray Diffraction technique:

In 1985 W.C. Rontgen discovered X-Rays diffraction technique. This technique is very useful for the study of crystal structure in detail. X-ray diffraction is rapid analytical technique for phase identification of crystalline structure, provides information for unit cell dimensions and atomic spacing .

x-ray diffraction technique relies on the dual nature i.e wave/particle nature of x-ray, which is used to study structure of crystals and degree of crystallinity of structure based on diffraction pattern. XRD gives us information on phases, structures, crystallographic orientation and various different parameters like crystal defects, average crystallite size, the structural strains and degree of crystallinity.

Various methods are there to determine the crystal structure like powder diffraction method, Laue method and rotating crystal method. Two methods used to determine size of crystal by powder diffraction method are as follows:

1. Diffractometer method.

2. Debye-Scherrer formula or method.

The sample to be studied is finely ground, different target materials like copper and molebdenum can be used. In our study, we have used XRD source of Cu-kα=1.54.

3.2.1 Working principle of XRD:

The powdered sample is used in this technique, when X-rays hit the surface of the powdered sample, the plane of the crystal on which it hits, acts as mirror and reflects the incoming x-ray or incident x-ray. The angle of incidence is equal to the angle of reflection for each set of atoms, which causes constructive interference with in the crystal. This phenomenon of interference can be explained on the basis of Bragg's law, it's equation is as follows:

$$n\lambda=2dSin\theta \quad \ldots\ldots\ldots\ldots\ldots\ldots\ldots\ldots \quad (3.1)$$

In this Bragg's law equation,

n=Interference order

λ=Wavelength of incident X-rays

d=Interlayer distance

θ=Angle of incidence

x-ray diffraction technique works on the principle of constructive interference as shown in fig 3.1, according to Bragg's law, if there are equally spaced planes and the X-ray radiation falls on them at distance 'd', then the rays reflected from these equally spaced planes have path difference equal to 2dSinθ, here θ is measured from the plane.[62]

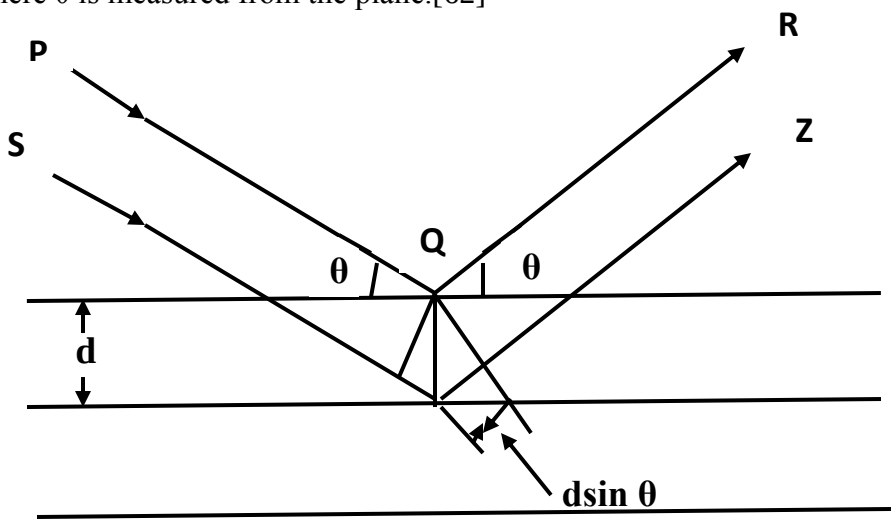

Fig. 3.1: Scattering of incident beams of x-rays at the plane of atoms in crystal

The condition for constructive interference is as follows:

$2d\sin\theta = n\lambda$ where n=1, 2, 3…..

In this above mentioned Bragg's equation, reflection happens only in the condition when $\lambda<2d$, this is the reason, visible light cannot be used, that's why X-rays are used. For characterization of three dimensional structures with the help of X-rays, three techniques are used, described as follows:

(i) Powder diffraction method

(ii) Laue Method

(iii) Rotating Crystal Method

As for XRD, the sample should be in powdered form and our sample is also a nanopowder and acceptable sized single crystals are not available, so, only powder diffraction method can be employed as suitable method in this technique. Before putting the sample in circular or rectangular, aluminium or glass plate, sample must be finely grinded. The X-rays are fallen on the sample, every nanoparticle acts as randomly oriented crystal.

If we consider one particular reflection plane, it can be seen that some of the nanoparticles from the sample are aligned in such a way that their hkl planes completely satisfies the conditions of Bragg's angle as shown in Fig. 3.2a. If θ is kept constant, then the reflected beam forms diffraction cone of radiation as shown in Fig. 3.2b. The interplanner spacing d can be calculated, if we exactly know the values of θ and λ.

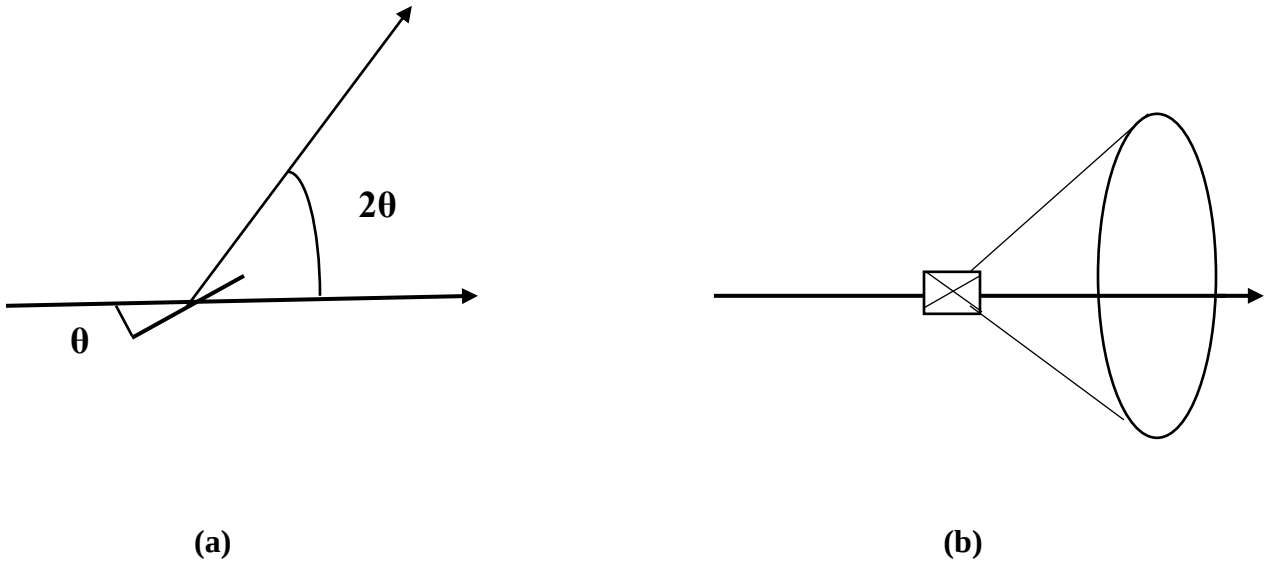

(a) **(b)**

Fig. 3.2a reflection plane satisfying Bragg's law

Fig. 3.2b diffracted cone of radiations in powder method

3.2.2 Lattice constant:

Lattice constant, also referred as lattice parameter can be defined as physical dimension of unit cell in a crystal lattice. In three dimensional lattices, three lattice constants are there referred as a, b and c as shown in Fig. 3.3. So, it is clear now that the length of

one of the edge of crystal lattice or angle between edges is actually the lattice constant. The equation used to calculate lattice constant is as follows:

$$a = \lambda (h^2+k^2+l^2)^{1/2} / 2\text{Sin}\theta \quad \ldots\ldots\ldots\ldots\ldots\ldots\ldots\ldots\ldots\ldots (3.2)$$

Where a denotes for the lattice constant, λ represents the wavelength of X-ray radiation (1.54 for Cukα), (h k l) are the miller indices and θ is the diffraction angle.

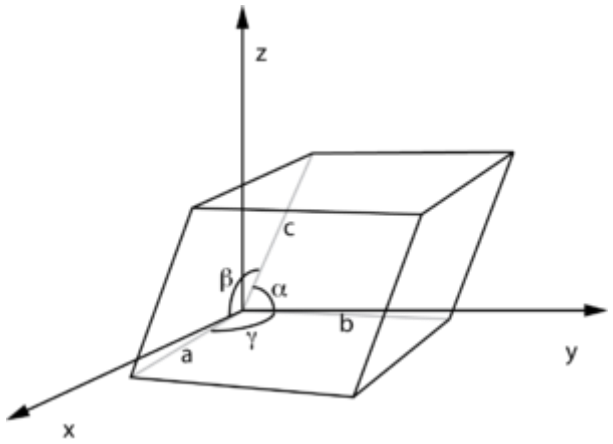

Fig 3.3 unit cell showing lattice constants [63].

3.2.3 Crystallite Size:

The crystallite size is a very important parameter as its value or magnitude influences other parameters also. For the confirmation of phase and its identification, diffractograms are compared to JCPDS or pdf cards. If diffractogram shows broad peaks, it refers to the presence of small crystallite size as Debye Scherrer equation gives us the inverse relation between peak width and crystallite size as shown below:

$$t = \frac{0.9\lambda}{\beta \cos\theta} \quad \ldots\ldots\ldots\ldots\ldots\ldots\ldots 3.3$$

Where "t" represents crystallite size, "λ" is the wavelength of the used X-rays, "θ" is the diffraction angle and "β" is FWHM value of respective peaks.

3.2.4 X-Ray Density:

The X-ray density can be calculated by the equation below, if value of lattice constant is known:

$$\rho_x = ZM / N_A a^3 \quad \ldots\ldots\ldots\ldots\ldots\ldots\ldots\ldots 3.4$$

Where "ρx" represents X-Ray density, "M" is Molecular weight of sample, "N_A" is Avogadro's number (6.022×10^{-23}) and "a" is lattice constant and "Z" is formula unit of cell. For spinel ferrite each unit cell has 8 formula units. X-ray density shows inverse proportionality with lattice constant and direct proportionality with molecular weight as shown in the above equation.

3.2.5 Bulk Density:

Bulk density, also named as measured density is calculated by simple conventional formula of density as shown below:

$$\rho_m = m/\pi r^2 h \quad \ldots\ldots\ldots\ldots\ldots\ldots\ldots\ldots 3.5$$

Bulk density depends on the internal structure of material i.e. it is intrinsic property of the material. Where "ρ_m" represents bulk density, "m" is mass, "r" denotes radius," h" is thickness of the pressed pellet sample. Circular pellets were made with the help of hydraulic press to calculate bulk density.

3.2.6 Porosity Fraction:

Porosity fraction is calculated if values of both X-ray density and bulk density are known, with the help of following equation:

$$\text{Porosity Fraction} = 1 - \rho_m / \rho_x \quad \ldots\ldots\ldots\ldots\ldots\ldots (3.6)$$

Where ρ_m is the bulk density and ρ_x is the X-Ray density of the sample.

3.3 Fourier Transformed Infrared Spectroscopy:

FTIR spectroscopy is a technique through which we get the absorption or emission spectrum of gas, liquid or solid. The FTIR spectrum obtained helps us to identify the materials by recognizing the chemical bonds and functional groups. The FTIR spectrophotometer is shown in Fig. 3.4.

Fig. 3.4: FTIR spectrophotometer [64].

3.3.1 Working Principle of FTIR:

FTIR is actually modified interferometer. Where a source emits a light directed into an interferometer, which processes the light, then the light moves into the compartment which contains sample and is then moved into the detector. The detector measures the signal and presents it as the interferogram, then it is processed by a complete algorithm known as Fourier Transformed Spectroscopy as shown in Fig. 3.5

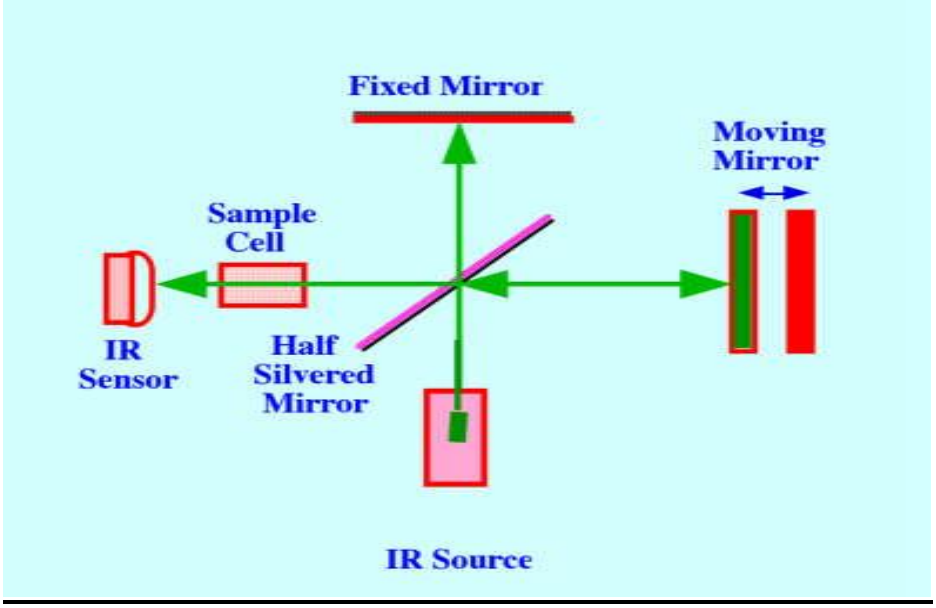

Fig. 3.5: Basic working principle of FTIR [64].

3.4 Scanning Electron Microscope:

SEM is a type of electron microscope that uses electron beam to scan surface of sample to produce image showing internal details. The image is created by scanning and collecting secondary electrons produced due to incident electron beam. The resolution of SEM is more than 1 nm. The SEM images gives us the detailed information about:

- Sample's composition
- Sample morphology / surface topography
- Phase mapping

Signals emitted from interaction of electron beam with matter includes secondary electron, back scattered electrons, transmitted electrons, cathodoluminesence and characteristic X-rays as shown in Fig. 3.6.

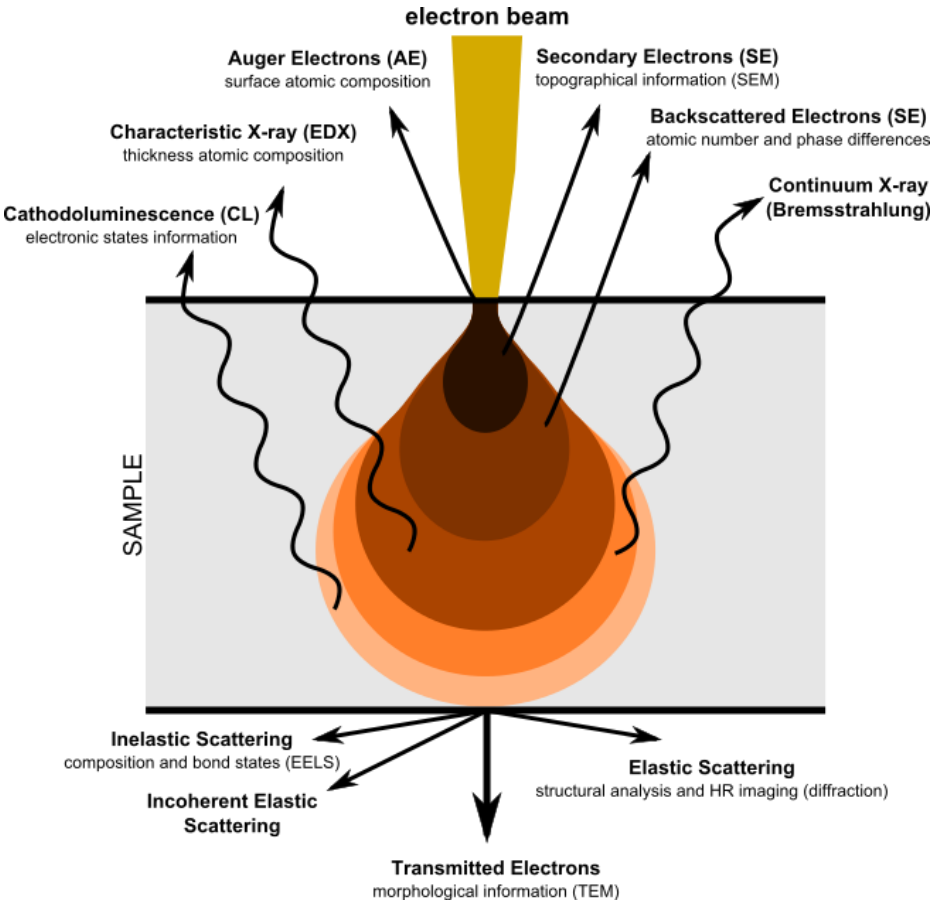

Fig. 3.6: Type of signals emitted from interaction volume [65].

3.4.1 Working Principle of SEM:

SEM can operate at low vacuum, high vacuum, series of temperatures and also in wet conditions. usually using raster scan in a narrow area ,the electron beam is focused on the sample utilizing magnetic lenses. During the beam passage from last lens, the beam is deflected in x and y direction, which enables us to control brightness of image. Electron beam comes in contact with the matter, interacts with it and produces various signals as shown in Fig. 3.6, these signals are detected by the different types of detectors.

Electron amplifiers amplify the signals, which is shown on screen as differences in brightness, as a result image is produced on cathode ray tube display. Three different types of images are produced by SEM: Secondary electron images, elemental X-ray maps and backscattered electron images.

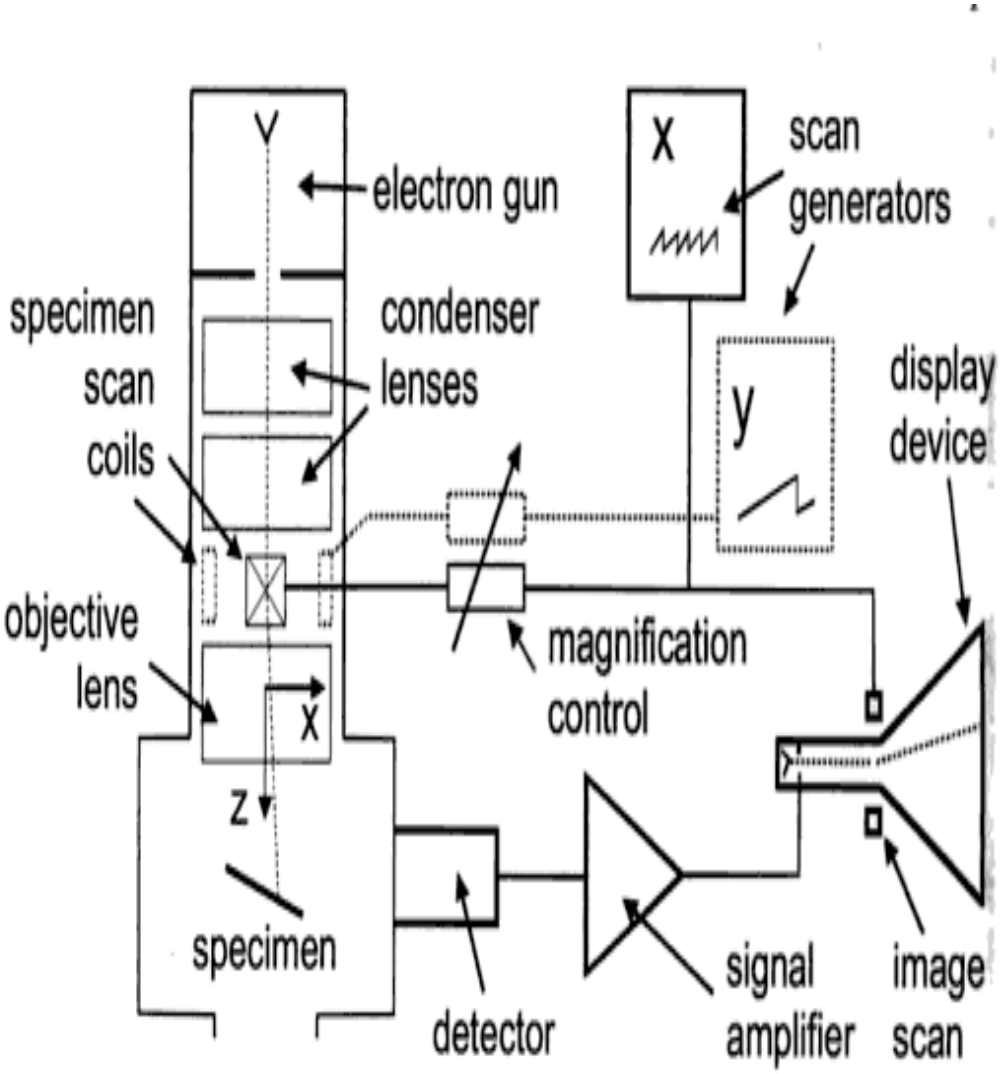

Fig. 3.7: Basic principle of SEM [66].

3.5 Dielectric Properties:

Wayne Kerr LCR 6500B was used to investigate in detail the dielectric properties (dielectric constant, dielectric loss and dielectric tangent loss). The dielectric constant Ɛ′ (real part) indicates charge storing capacity and tendency of polarization. LCR meter was used to measure capacitance and d-factor and then by using the formula given below, dielectric constant was calculated:

$$\varepsilon' = C \times t / (A\, \varepsilon^0) \qquad \text{…….. (3.6)}$$

Where C denotes the capacitance of the pellet measured in farad, t represents the thickness of the pellet measured in meters, A is the cross-sectional area of the flat surface of the pellet and ε_0 is the constant of permittivity for free space and is equal to 8.85×10^{-12} F/m.

The dielectric loss Ɛ″ (imaginary part) indicates the energy loss or in other words, energy dissipation. The dielectric loss is calculated by the equation given below:

$$\varepsilon'' = \varepsilon' \tan\delta \qquad \text{…….. (3.7)}$$

Dielectric loss tangent factor (tan δ) is the ratio of dielectric loss to dielectric constant and it can also be defined as ratio of the resistive current to the charging current. It actually measures the relative energy loss with respect to changing field of AC. It is calculated by the equation given below:

$$\tan\delta = \varepsilon'' / \varepsilon' \qquad \text{…….. (3.8)}$$

The dielectric parameters can be explained in accordance with Maxwell-Wagner model and Koop's theory.

3.6 AC Conductivity:

AC conductivity is the physical property of the material, which gives us the insight about the electrical conductivity of the material, hopping is the phenomenon which mainly describes the conductivity in ferrites [67]. AC conductivity is measured over a frequency range of 100 Hz to 5 MHz frequency at room temperature. It is calculated by the equation given below:

$$= \omega \varepsilon^0 \varepsilon' \tan\delta \qquad \text{…….(3.9)}$$

Where σ_{AC} represents the AC conductivity, ε^0 is permittivity of free space, ε' is dielectric constant and tan δ is dielectric loss tangent. The SI unit of AC conductivity is S/m.

3.7 AC impedance spectroscopy:

The real and imaginary parts of impedance are extensively studied to explore the variation of AC impedance with respect to frequency in electro ceramic materials. Reactance (X) and resistance (R) are measured over a range of 100 Hz to 5 MHz in present study. For our sample, the AC impedance parameters are measured at room temperature.

The real part [resistance (R)] and imaginary part [Reactance (X)] of impedance relates with each other to form complex impedance (Z) expressed in the form of equation below:

$$Z = R + jX \quad \text{.....(3.10)}$$

The SI unit of impedance is 'Ω'. The Cole-Cole plot of real and imaginary parts of impedance shows contribution of resistance in the material.

Chapter 4

Results and Discussion:

4.1 X-ray Diffraction (XRD) Results:

X-ray diffraction technique is considered very useful in the detailed study of crystal structure, this technique proves highly beneficial in confirming the formation of desired material.

It was used to check the cell dimensions, phase formation and crystalline structure of the synthesized Nickel ferrite nanoparticles and its nanohybrid with Carbon nanofibers.

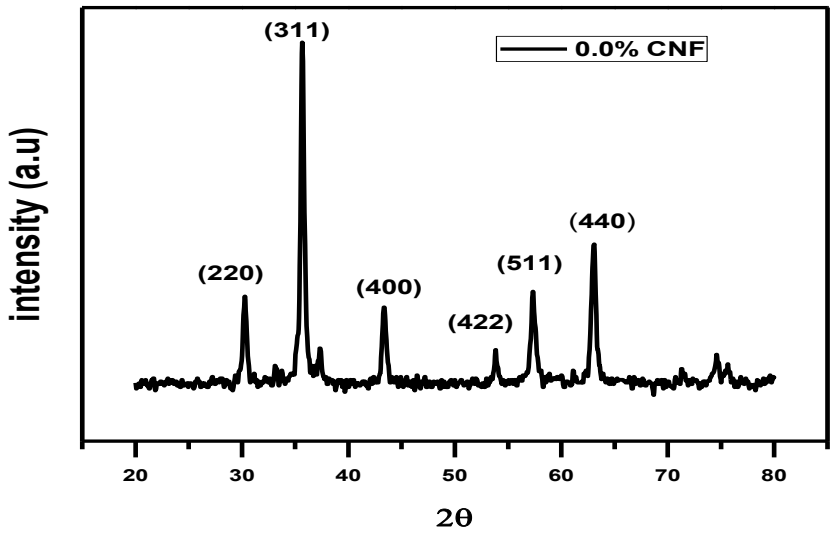

Fig. 4.1: XRD of pure Nickel Ferrite (0.0% CNFs)

Fig. 4.1 shows the diffractogram of pure Nickel ferrite nanoparticles calcinated at 800 ^{o}C for 6 hours. These nanoparticles were synthesized using wet co-precipitation method. The XRD pattern confirms the synthesis of the face centered cubic structure in accordance with JCPDS Card no.01-

088-0380, showing space groups Fd3m at 2θ as shown in Table 4.1.The sample contained no impurity peak with in x-ray detection range. The XRD pattern shows peaks at reflection planes (220), (311), (400), (422), (511) and (440) as shown in Fig. 4.1. The crystallinity of the synthesized product was assured by the presence of most intense peak at $2\theta = 35.650^{o}$ on the respective plane (311) and the formation of small grain and crystallites sizes was assured by the obtained values of the FWHM. The average crystallite size was found to be 24.5 nm. No other peak was observed showing the complete absence of all type of impurities.

Table 4.1: shows the peak position (2θ) of the reflection planes of the $NiFe_2O_4$/CNFs nanohybrid as a function of CNFs contents (weight %).

CNFs Concentration	2θ at (220)	2θ at (311)	2θ at (400)	2θ at (422)	2θ at (511)	2θ at (440)
0.0%	30.204°	35.670 °	43.317 °	53.835°	57.346 °	63.058°
10%	30.241°	35.650 °	43.304°	53.810°	57.413°	62.993°
15%	30.201°	35.628°	43.650°	53.876°	57.358°	62.990°
20%	30.327°	35.676°	43.412°	53.854°	57.475°	63.088°

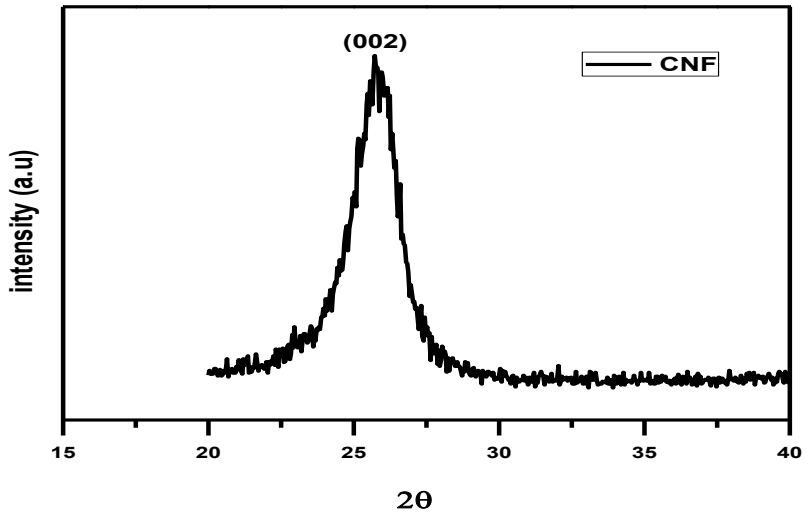

Fig. 4.2: XRD of the CNF.

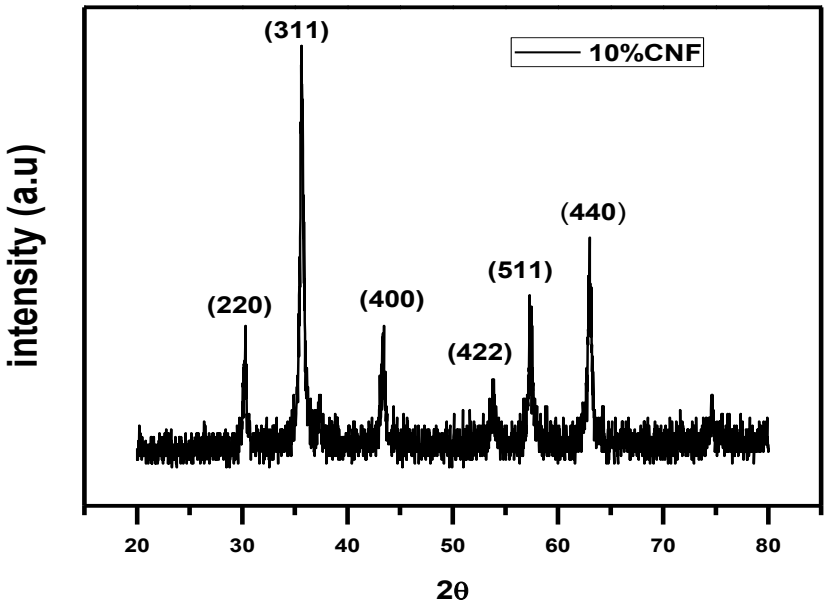
(311)
10%CNF
(440)
(511)
(220)
(400)
(422)
intensity (a.u)
20
30
40
50
60
70
80
2θ

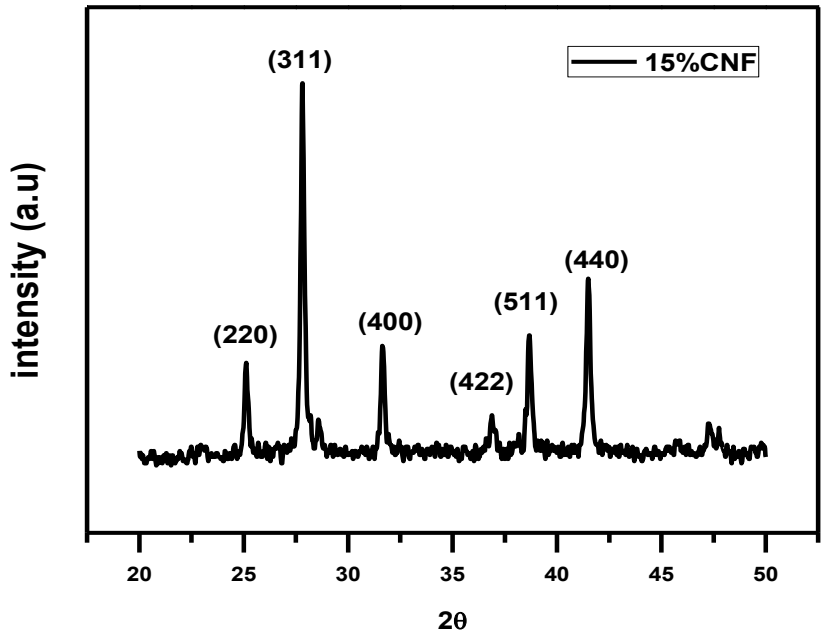
(311)
15%CNF
(440)
(511)
(220)
(400)
(422)
intensity (a.u)
20
25
30
35
40
45
50
2θ

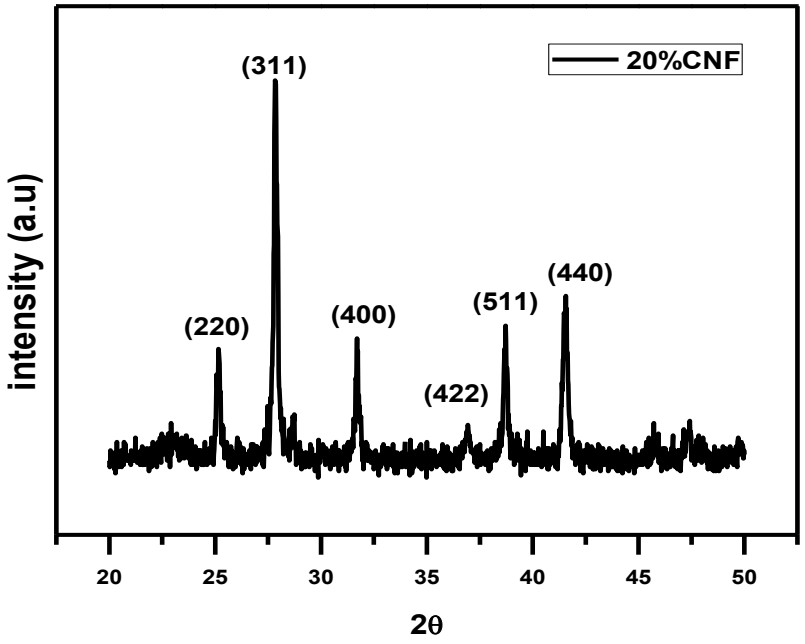

Fig. 4.3: XRD of the $NiFe_2O_4$/CNFs nanohybrids with increasing CNF weight percent.

XRD was used to check the formation of the desired synthesized product i.e. $NiFe_2O_4$ /CNF and its phase formation. Fig. 4.2 shows diffractogram of pure CNFs. Fig. 4.3 illustrates the diffractograms of $NiFe_2O_4$/CNF (10%, 15% and 20%) obtained at room temperature. All the samples showed well resolved distinct peaks at reflection planes (220), (311), (400), (422), (511) and (440). The sample contained no impurity peak with in x-ray detection range.

The characteristic peak (002) showing graphitic reflection at $2\theta = 26^o$ [39, 61] is not shown in any diffractogram indicating uniform distribution, single phase formation and complete anchorage of $NiFe_2O_4$ on all CNF. The average crystallite size was found to be in the range of 28±4 nm, calculated by using Debye-Scherrer equation [26] [68] as shown in Table 4.2.

Table 4.2: Shows the variation of average crystallite size ($t_{(average)}$ in nm), lattice parameter (a in Å), molecular density (Dm in g/cm3), X-ray density (Dx in g/cm3), volume of cell (Vcell), Porosity (fraction) of the $NiFe_2O_4$/CNFs nanohybrid as a function of CNFs contents (weight %).

MWCNTs Concentration	**0.0%**	**10%**	**15%**	**20%**
$t_{(average)}$ (nm)	**24.5**	**30.2**	**31.412**	**32.798**
a (Å)	**8.34**	**8.35**	**8.35**	**8.35**
Dm (g/cm3)	**3.107**	**3.63**	**4.24**	**5.09**
Dx (g/cm^3)	**5.369**	**5.377**	**5.39**	**5.41**
Vcell (a3)	**580.09**	**582.18**	**582.18**	**582.18**
P (fraction)	**0.421**	**0.3241**	**0.214**	**0.058**

The lattice constant as described in chapter 3 is essential for studying the dimensions of unit cell of crystal. Lattice constants of samples were measured by using equation 3.2 mentioned in chapter 3 as mentioned in Table 4.2, its trend with increasing CNFs is shown in Fig. 4.3.

The crystallite size was calculated using equation 3.3 mentioned in chapter 3, it showed increasing trend with the increase in carbon nanofibers contents in the nanohybrid as shown in Fig. 4.5. This increase is well in agreement with values of FWHM. The average crystallite size was found to be in the range of 28±4 nm, calculated using Debye-Scherrer's equation [26, 68] as shown in Table 4.2.

The ratio of mass of unit cell to the volume of unit cell is referred as X-ray density and the ratio of mass of solid to the volume of solid is referred as mass density or bulk density.

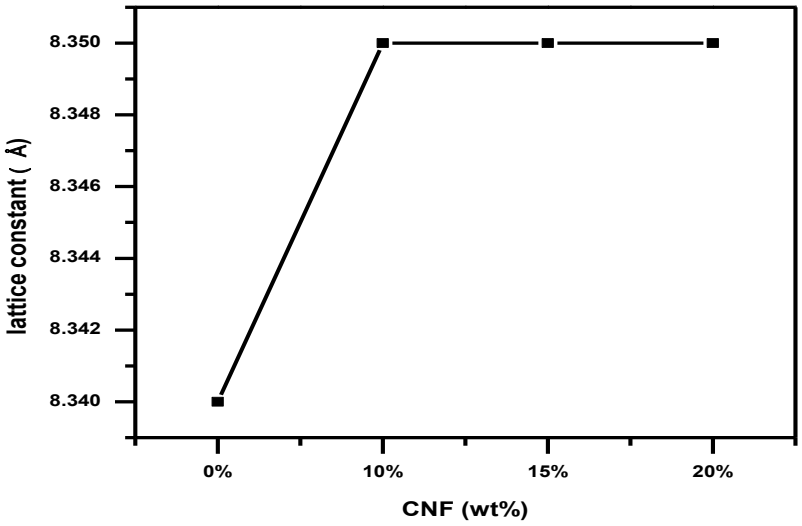

Fig. 4.4: Trend of lattice constant of $NiFe_2O_4$/CNFs nanohybrid as a function of CNFs content (weight %)

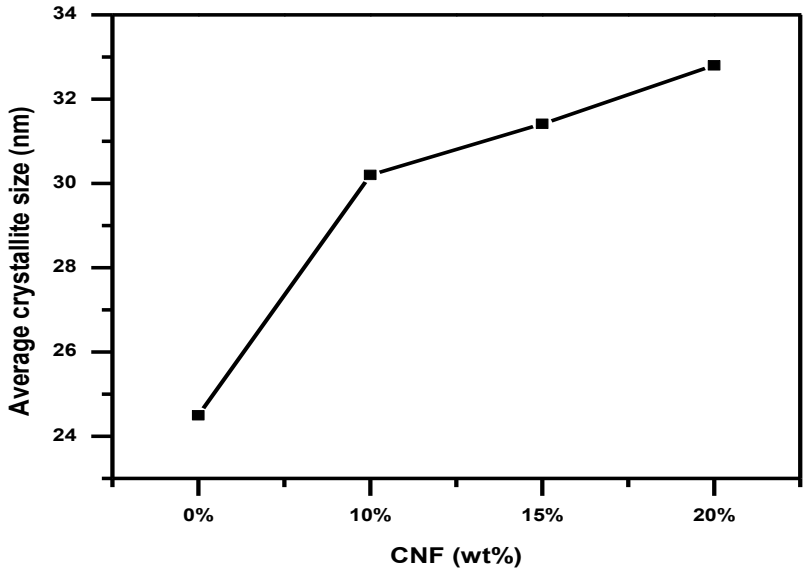

Fig. 4.5: Trend of crystallite size of $NiFe_2O_4$/CNFs nanohybrid as a function of CNFs content (weight %)

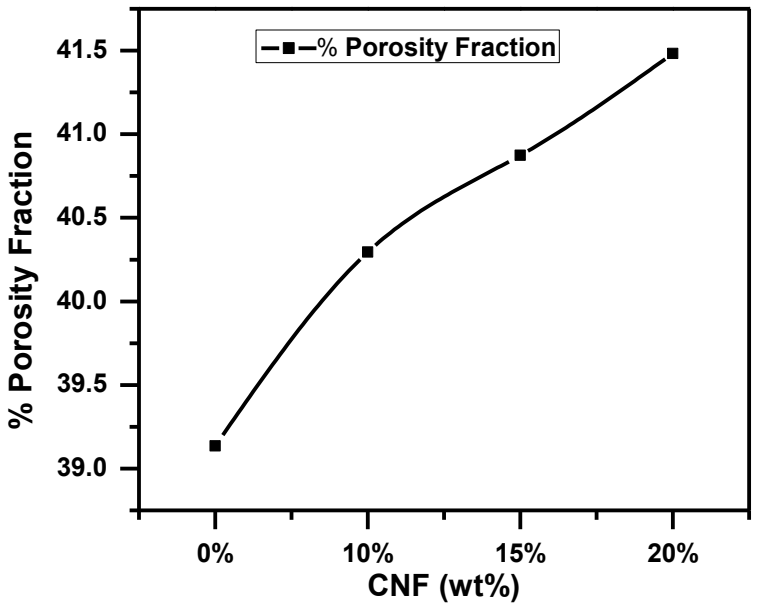

Fig. 4.6: Trend of porosity fraction of $NiFe_2O_4$/CNFs nanohybrid as a function of CNFs content (weight %)

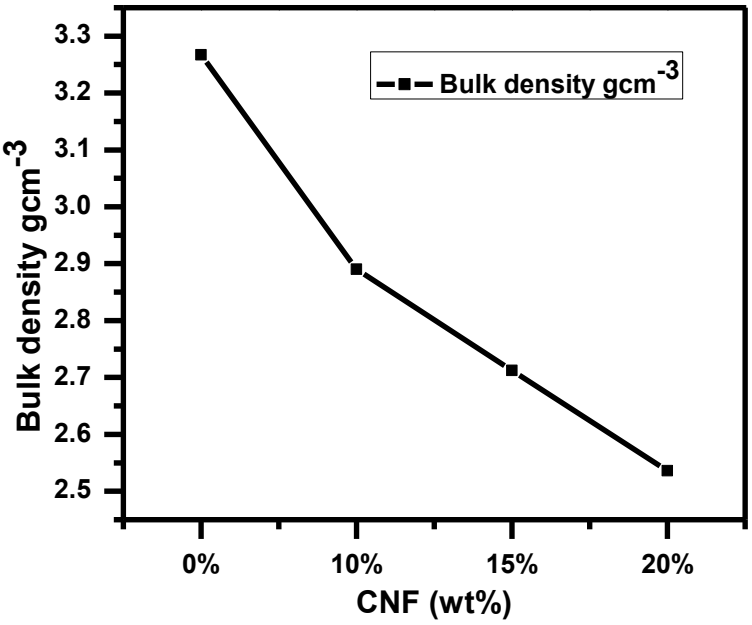

Fig. 4.7: Trend of bulk density of $NiFe_2O_4$/CNFs nanohybrid as a function of CNFs content (weight %)

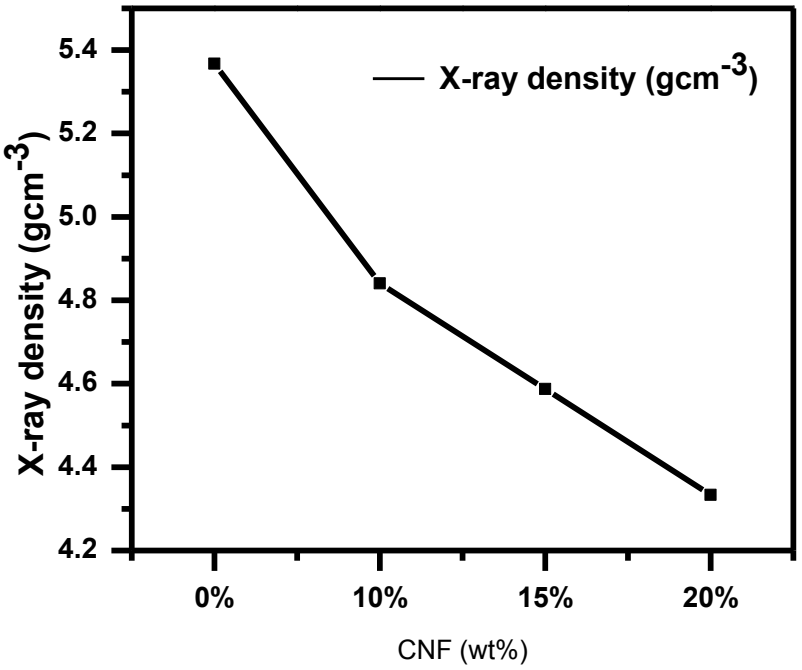

Fig. 4.8: Trend of X-ray density of $NiFe_2O_4$/CNFs nanohybrid as a function of CNFs content (weight %)

Fig. 4.7 & 4.8 clearly shows the continuous decrease of bulk density and X-ray density on addition of CNFs. This is mainly due to the light weight and highly porous nature of Carbon nanofibers. Due to carbon nanofibers having low mass and more volume, the decrease in bulk and X-ray density are as expected. Fig. 4.6 shows the increasing trend of porosity. The introduction of carbon nanofibers created more and more interfaces in nickel ferrite matrix and eventually more defects causing increase in porosity of hybrid as expected. The overall parameters are shown in Table 2.

4.2 SEM Results:

Scanning electron microscopy was used to check the structure, morphology of the product and also the size of nanoparticles was confirmed. The samples of SEM were prepared by sonicating the powder of the samples in distilled water for one hour, to break the clusters, if any are present. Fig. 4.9 shows the well dispersed and uniformly distributed Nano sized nickel ferrites particles, the size of nanoparticles is well in agreement with and confirms the results of XRD data. Fig. 4.10

shows the Carbon nanofibers. Fig. 4.11, 4.12, 4.13, 4.14 demonstrates the anchorage of $NiFe_2O_4$ on carbon nanofibers at different magnifications, showing complete covering of carbon nanofibers with $NiFe_2O_4$ nanoparticles, which proves the efficiency of our novel method. Small sized clusters of nanoparticles can be seen, their presence can be attributed to weak Vander walls forces, Brownian motion and less repulsive forces [69]. The formation of agglomerates can also be explained in accordance with dipolar nature of magnetic nickel ferrite nanoparticles [68].

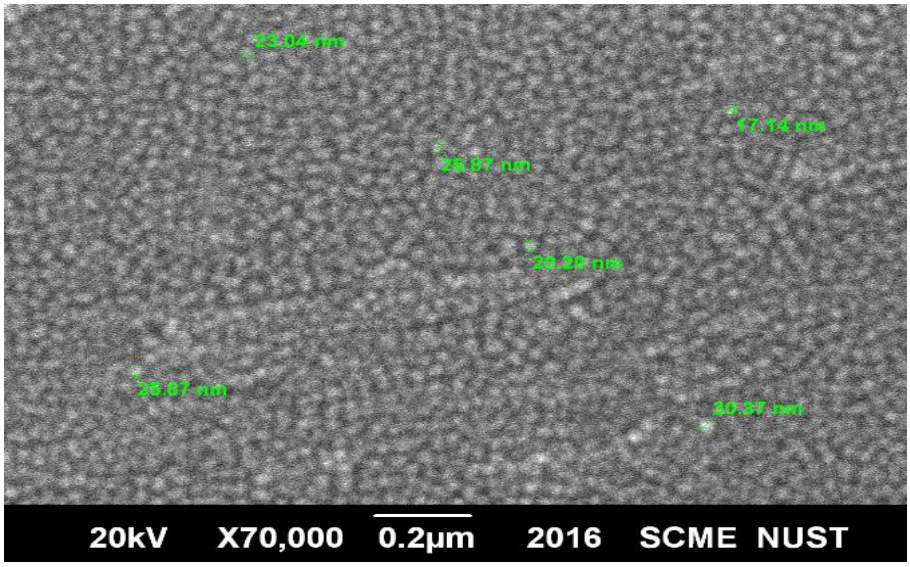

Fig. 4.9: SEM image of pure $NiFe_2O_4$

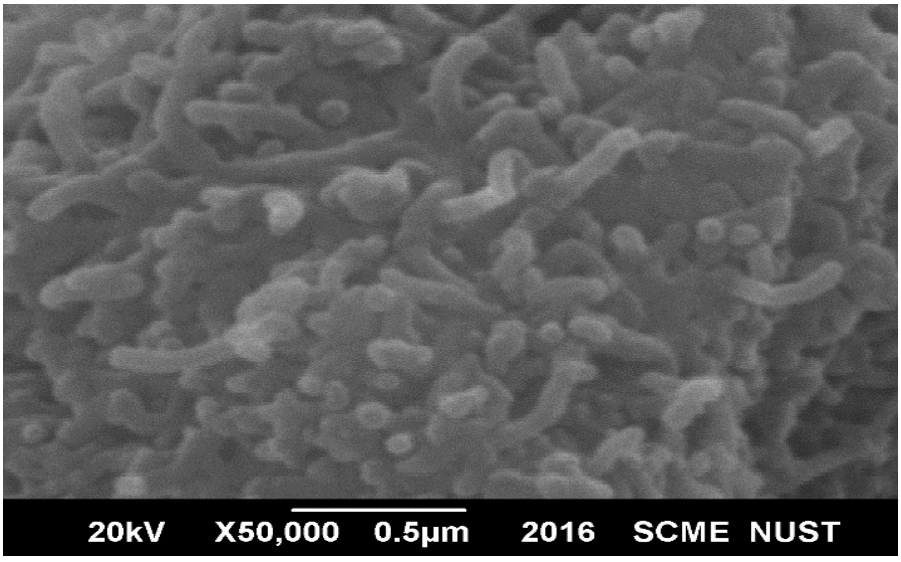

Fig. 4.10: SEM image of pure CNF

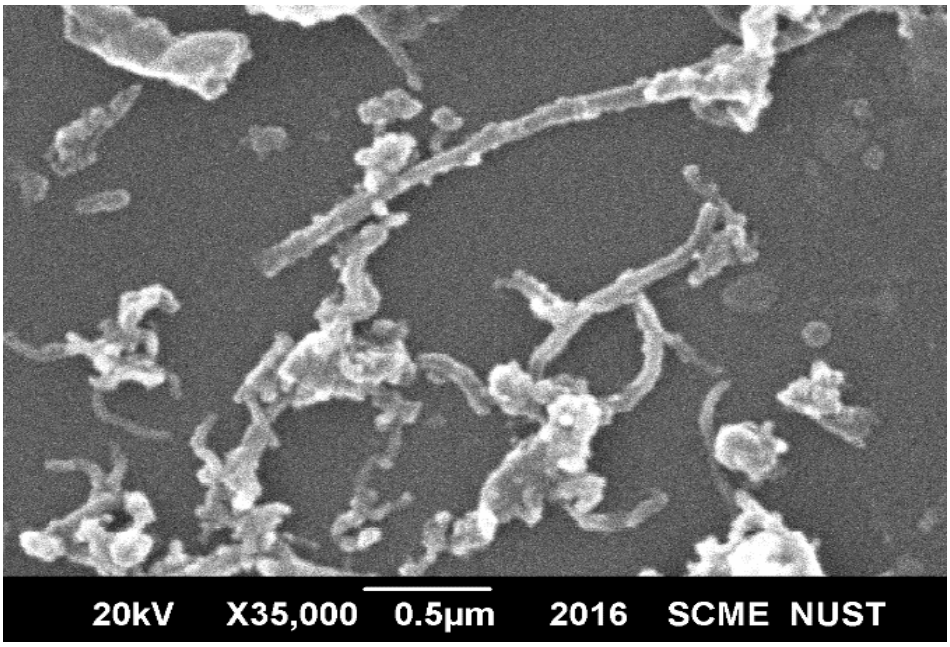

Fig. 4.11: SEM image of $NiFe_2O_4$/CNFs nanohybrid with 20% CNFs at 35000 X

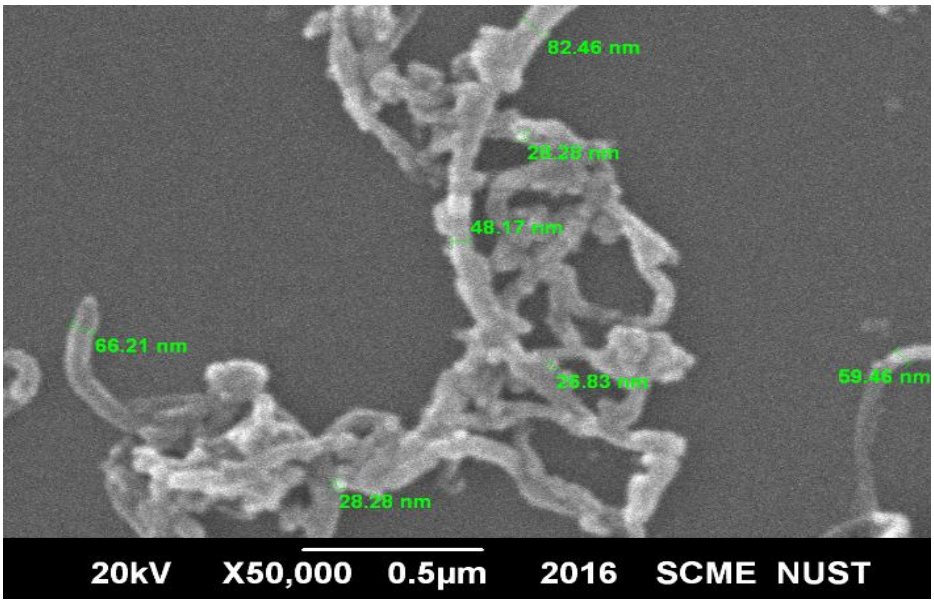

Fig. 4.12: SEM image of $NiFe_2O_4$/CNFs nanohybrid with 20% CNFs at 50,000 X

.

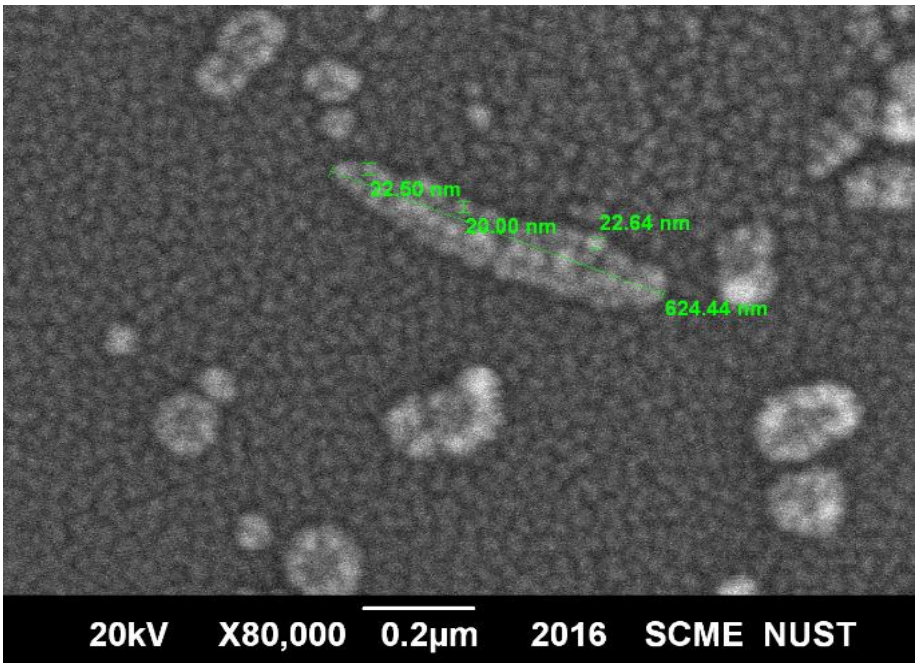

Fig. 4.13: SEM images of $NiFe_2O_4$/CNFs nanohybrid with 20% CNFs at 80,000 X

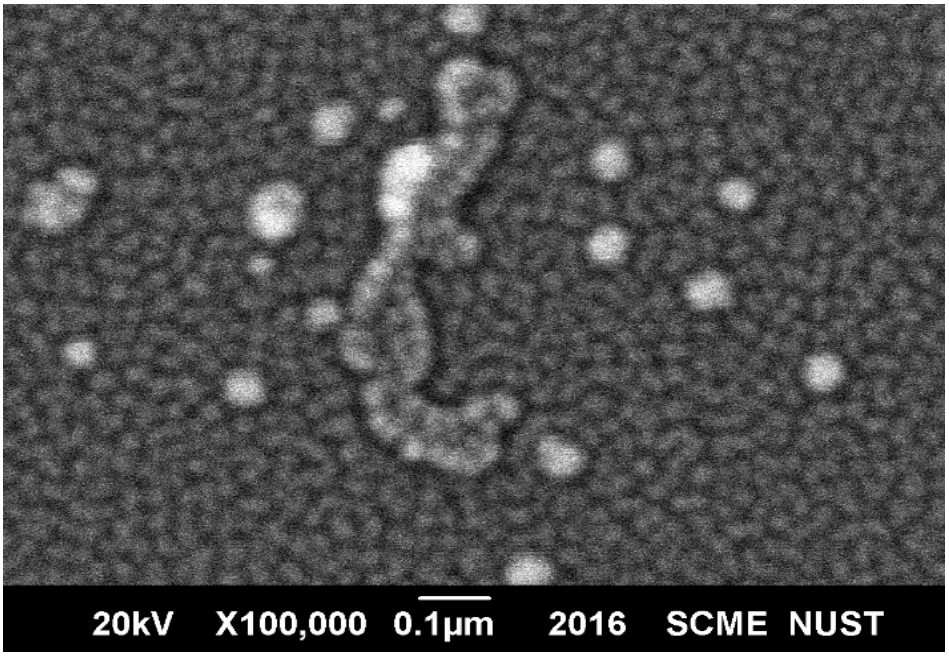

Fig. 4.14: SEM images of $NiFe_2O_4$/CNFs nanohybrid with 20% CNFs at 100,000 X.

4.3 FT-IR Spectroscopy:

Infrared radiations are used in this spectroscopy. Three divisions of infrared spectrum is there described as follows:

a. Near infrared region (12800~4000 cm^{-1})
b. Mid infrared region (4000~200 cm^{-1})
c. Far infrared region (50~1000 cm^{-1}).

We obtained results in the mid infrared region in the range of 400 to 1000 cm^{-1}.The FTIR spectroscopic analysis (described in detail in chapter 3) of $NiFe_2O_4$ and $NiFe_2O_4$/CNF (10%, 15% and 20%) was done at room temperature in the range of 350 cm^{-1} to 4000 cm^{-1}. The samples for FT-IR were prepared at 4 tons of pressure for 3 minutes in hydraulic press by using KBr.

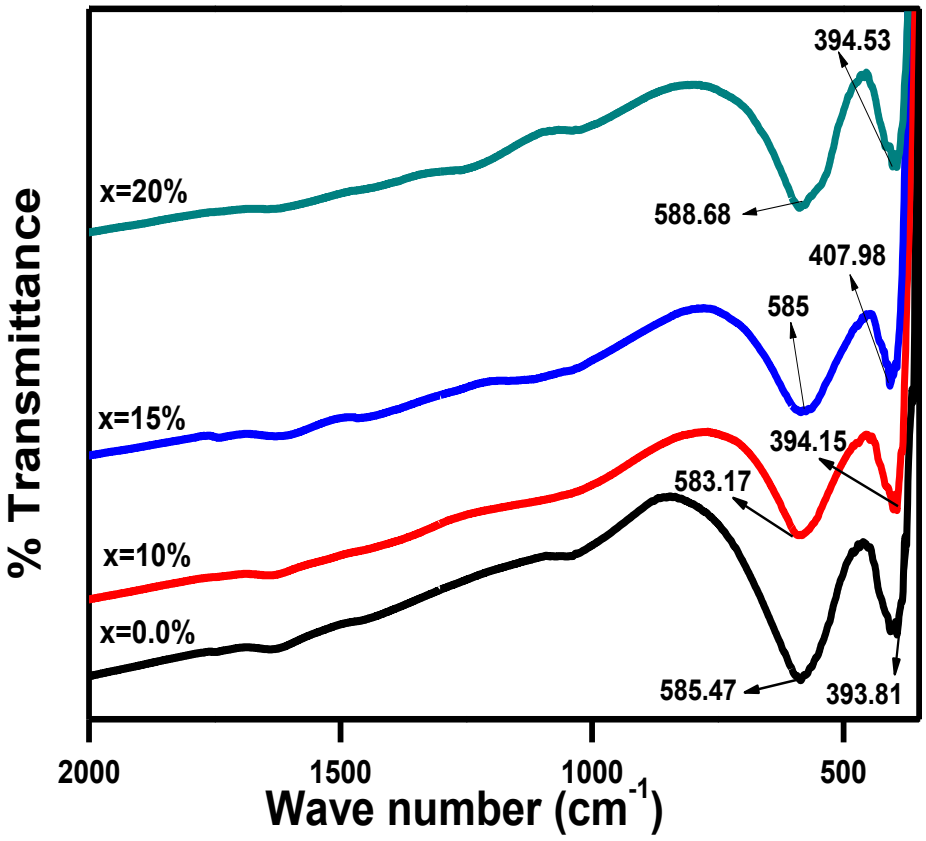

Fig. 4.15: FT-IR spectra for pure $NiFe_2O_4$ and synthesized $NiFe_2O_4$/CNFs nanohybrid as a function of CNFs contents (weight %).

Table 4.3: Shows the Tetrahedral (A) and Octahedral (B) band positions for $NiFe_2O_4$/CNFs nanohybrid.

CNFs Concentration	0.0%	10%	15%	20%
ν_1	585.47	583.17	585.00	588.68
ν_2	393.81	394.15	583.17	394.53

Fig. 4.15 shows nearly same spectra for all samples which refers towards the presence of same chemical bonds. Generally two sharp characteristic peaks or absorption bands are observed in FTIR spectra of spinel ferrites. The metal ion stretching vibrations mostly observed at higher frequencies absorption band (ν_1) ranging from 600-550 cm^{-1} corresponds to tetrahedral sites, whereas metal ion stretching at comparatively lower frequencies absorption band (ν_2) ranging from 450-385 cm^{-1} corresponds to octahedral sites [41]. In present work, all spectra shows the peaks around 390-408 cm^{-1} and 583-588 cm^{-1} representing the octahedral and tetrahedral sites respectively as shown in Table 4.3. The Fe-O bond lengths differences at octahedral and tetrahedral sites can be held responsible for the differences in ν_1 and ν_2 absorption bands [61]. The observed peaks are well supported by the previously reported results [18, 41, 61, 68, 70-73] which confirms the synthesis of desired product.

4.4 Dielectric properties:

The dielectric constant ε' (real part) indicates charge storing capacity and tendency of polarization. Pure $NiFe_2O_4$ has dielectric constant of 1.79×10^3 at 100 Hz, which decreases to 23.4 at 5 MHz. The large values of dielectric constant at lower frequencies can be attributed to the presence of all type of polarizations including electronic, ionic and space charge. This space charge polarization is more at high temperature and low frequency. The decrease in dielectric constant with increase in frequency can be explained with the help of Koop's theory. According to which dielectric material is considered as Maxwell-Wagner type medium of two layers in which the conducting grains of dielectric material are separated by the insulating

grain boundaries. At lower frequencies, electron reach at grain boundaries by hopping, accumulates there and as a result produces high permittivity but at higher frequencies the electrons start moving in opposite direction due to which they do not reach at grain boundaries, thus decreasing dielectric constant [26, 29, 74]. Due to the addition of CNF's, the huge enhancement of dielectric properties is observed. As for 20% addition of CNF's the dielectric constant measured came out to be 2.92 x 10^6 at 100 Hz as shown in Fig. 4.16. This increase can be attributed to the conductive nature of CNF's and Maxwell and Wagner model of space-charge polarization [74, 75]. The conductive network of carbon nanofibers act as parallel plate capacitor in the ferritic matrix, thus increasing the capacity of the system to store charge generated due to the polarization of Maxwell and Wagner type medium of ferrite.

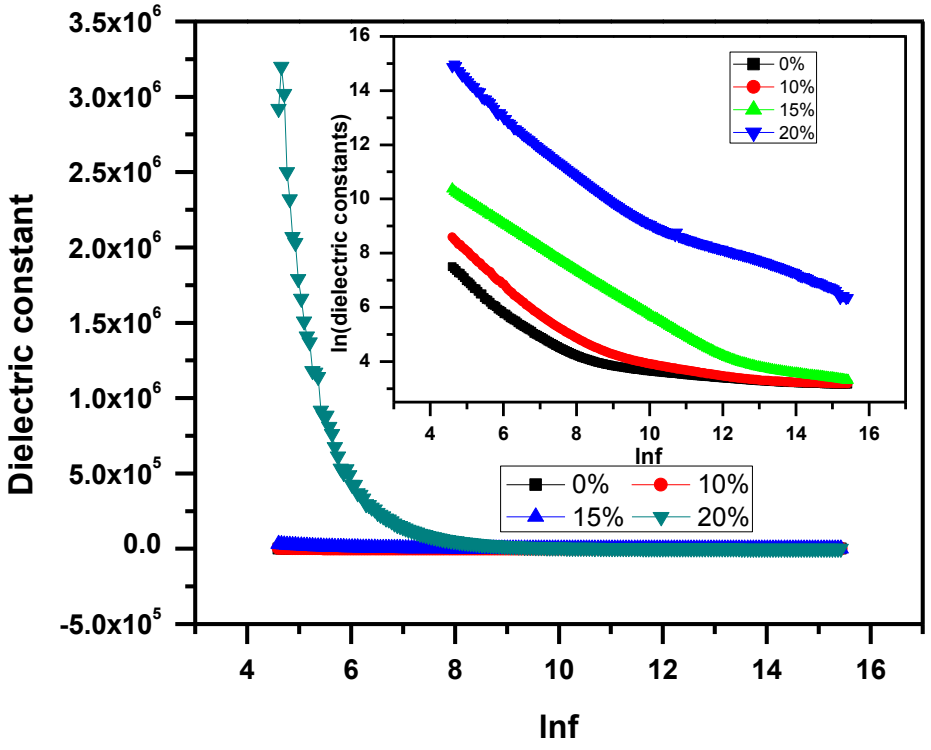

Fig. 4.16: Trend of dielectric constant with frequency for $NiFe_2O_4$/CNFs nanohybrid as a function of CNFs contents (weight %).

The dielectric loss Ɛ″ (imaginary part) indicates the energy loss or in other words, energy dissipation. The dielectric loss is showing exactly the same trend as of dielectric constant. Pure $NiFe_2O_4$ has dielectric loss of 6.21 x 10^3 at 100 Hz, which decreases to 0.902 at 5 MHz. By the

addition of CNF's, there is an increase in values of dielectric loss as shown in Fig. 4.17. For 20% CNF's concentration showed maximum of 7.65 x 10^6 at 100 Hz. This increase in dielectric loss can be attributed to the presence of defects and voids created at the interfaces of nickel ferrite and CNFs network and also to the space charge polarization theory, according to which, well conducting grains are present in dielectric structures, these grains are separated by very thin, resistive and poorly conducting grain boundaries. When electric field is applied, hopping electrons between Fe^{+2} and Fe^{+3} gets accumulated at grain boundaries and causes voltage drop as more energy is required for hopping due to the high resistivity of grain boundaries causing greater energy loss. As frequency increases, the hopping of electrons between Fe^{+2} and Fe^{+3} ions experiences less resistance due to the low resistivity of conducting grains and as a result low energy loss and dielectric loss values are observed. All this is also in agreement with Koop's theory, which states that the grain boundary effect is more evident at low frequencies [67]. At high frequencies, hopping of electrons do not follow the changes in applied field after a certain limit, which makes the values of dielectric constant and dielectric loss to get constant.

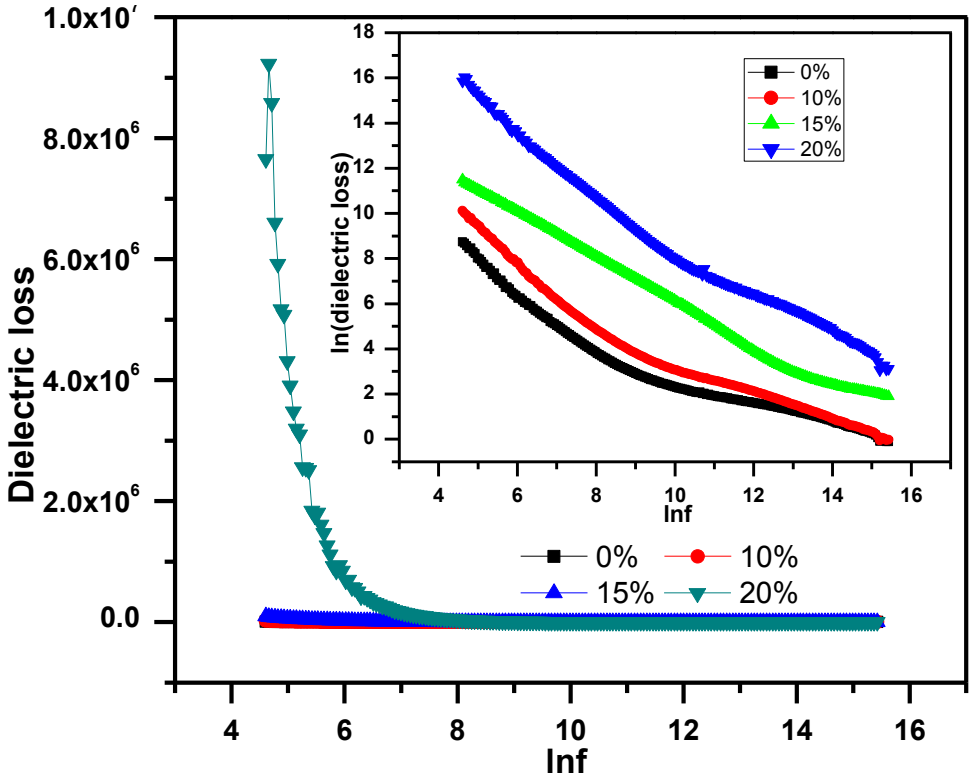

Fig. 4.17: Trend of dielectric loss with frequency for $NiFe_2O_4$/CNFs nanohybrid as a function of CNFs contents (weight %).

Dielectric loss tangent factor (tan δ) is the ratio of dielectric loss to dielectric constant and it can also be defined as ratio of the resistive current to the charging current. It actually measures the relative energy loss with respect to changing field of AC. In this work it shows the decreasing trend with increasing frequency. As Pure $NiFe_2O_4$ has dielectric loss tangent factor (tan δ) of 2.62 at 100 Hz and decreases to 3.86 x 10^{-2} at 5 MHz. The trend shows good match to the findings of Koop's theory and can also be explained that is at low frequency due to grain boundaries (high resistivity region), more energy is needed for exchange of electrons between Fe^{+2} and Fe^{+3} ions present at octahedral sites, that's why dielectric loss tangent factor (tan δ) is high at low frequency but at high frequency due to presence of grains (low resistivity region) electron exchange becomes relatively easy between Fe^{+2} and Fe^{+3} ions, thus lowering tangent loss values [67].

Dielectric loss tangent shows increasing trend on increasing the percentage content of CNFs in the $NiFe_2O_4$/CNF hybrid. For 20% $NiFe_2O_4$/CNF hybrid, dielectric loss tangent factor (tan δ) was measured to be 4.67 at 100 Hz and decreased to 2.43 x 10^{-1} at 5 MHz. Relative more energy loss at low frequencies can be attributed to more interruption to flow of electrons. Fig. 4.18 shows the variation trends of dielectric loss tangent factor (tan δ).This shows that with increasing frequency, the energy loss decreases and becomes stagnant afterwards, this behavior at high frequency proves this $NiFe_2O_4$/CNF hybrid of having applications in high frequency microwave devices.

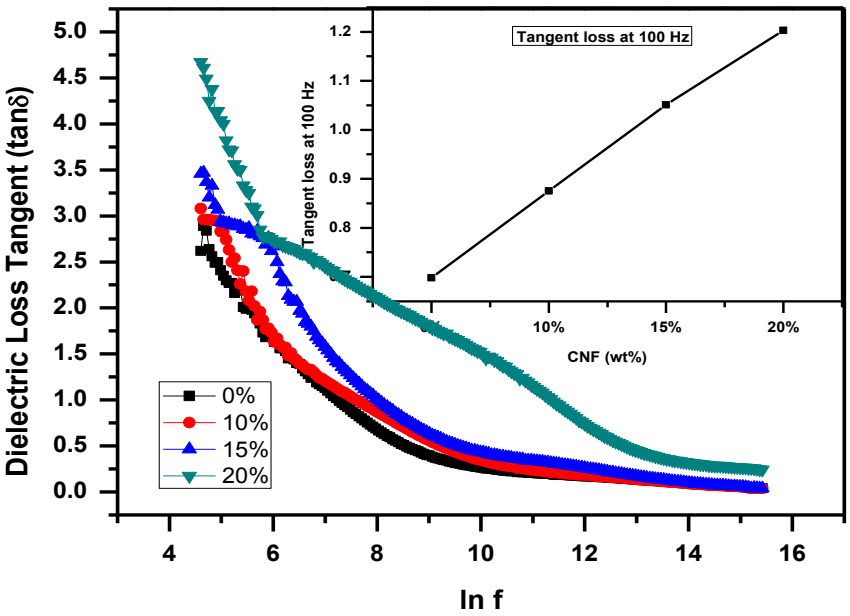

Fig. 14.18: Trend of dielectric loss tangent with frequency for $NiFe_2O_4$/CNFs nanohybrid as a function of CNFs contents (weight %).

4.5 AC Conductivity:

AC conductivity is the physical property of the material, which gives us the insight about the electrical conductivity of the material, hopping is the phenomenon which mainly describes the conductivity in ferrites [67].

Table 4.4: shows the variation of AC conductivity (σAC),dielectric tangent loss (Tanδ), dielectric constant (ε′),dielectric loss (ε″) of $NiFe_2O_4$/CNFs Nano hybrid as a function of CNFs contents (weight %).

MWCNTs Concentration	0.0%	10%	15%	20%
σAC (100 Hz)	3.45×10^{-5}	1.38×10^{-4}	5.47×10^{-4}	1.62×10^{-2}
σAC (1 MHz)	2.51×10^{-4}	2.71×10^{-4}	1.85×10^{-3}	1.59×10^{-1}
Tanδ (100 Hz)	2.62	3.08	3.46	4.67
Tanδ (1 MHz)	3.86×10^{-2}	3.89×10^{-2}	4.06×10^{-2}	2.43×10^{-1}
ε′ (100 Hz)	1790	5340	31900	2.92×10^{6}
ε′ (1 MHz)	23.4	24.1	27.4	574
ε″ (100 Hz)	6210	24900	98300	7.65×10^{6}
ε″ (1 MHz)	0.902	0.976	6.65	22.6

AC conductivity shows the increasing trend with increasing percentage of CNF at low frequencies which can be attributed to the increase in band conduction in comparison to hopping conduction due to the addition of conductive CNFs. At 100 Hz frequency the pure $NiFe_2O_4$ shows lowest AC conductivity value of 3.45 $x10^{-5}$ S/m while 20% hybrid shows highest AC conductivity value of 0.0162 S/m as shown in Table 4.4.

It can be seen in Fig. 4.19 that at low frequency AC conductivity decreases but again increases at high frequency, this trend can be explained on the basis of polarons, with increase in frequency

AC conductivity decreases in large polaron hopping and in small polaron hopping, AC conductivity increases with increase in frequency [76, 77]. In general, AC-conductivity increases with increasing CNFs concentration.

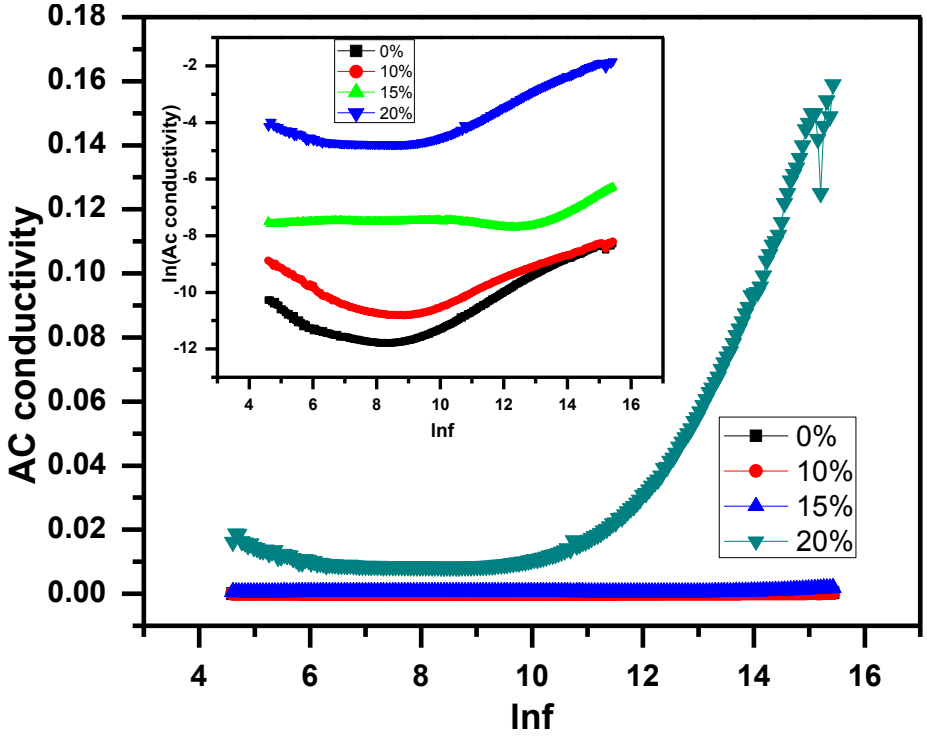

Fig. 4.19: Trend of AC conductivity with frequency for $NiFe_2O_4$/CNFs nanohybrid as a function of CNFs contents (weight %).

4.6 AC impedance spectroscopy:

The real and imaginary parts of impedance are extensively studied to explore the variation of AC impedance with respect to frequency in electro ceramic materials. The AC impedance parameters have shown the drastic change with increase in percentage of CNFs in the $NiFe_2O_4$/CNF hybrid. Fig. 4.19 shows the decreasing trend of AC impedance with increase in frequency as a function of increasing percentage of CNFs in the $NiFe_2O_4$/CNF hybrid. This decrease in impedance on addition of CNFs can be explained in light of conductive nature of CNFs. The phenomenon of decrease in resistance and reactance is observed due to the formation of conductive network of CNFs in the vicinity of grain boundaries, due to

which the value of resistance decreases near grain boundaries with increasing percentages of CNFs as shown in Fig. 4.21 & 4.22 respectively. The pure $NiFe_2O_4$ has highest impedance values of 5.89 $x10^7$ Ohm at 100 Hz and $NiFe_2O_4$/CNF Nano hybrid with 20% CNFs concentration has the lowest impedance values of 4.253 $x10^3$ Ohm at 5 MHz.

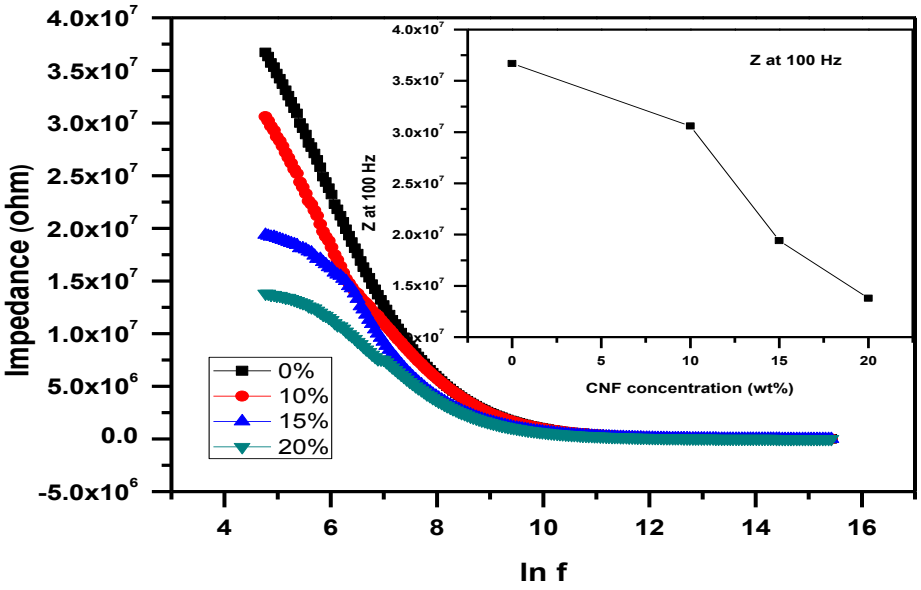

Fig. 4.20: Trend of Impedance with frequency for $NiFe_2O_4$/CNFs nanohybrid as a function of CNFs contents (weight %).

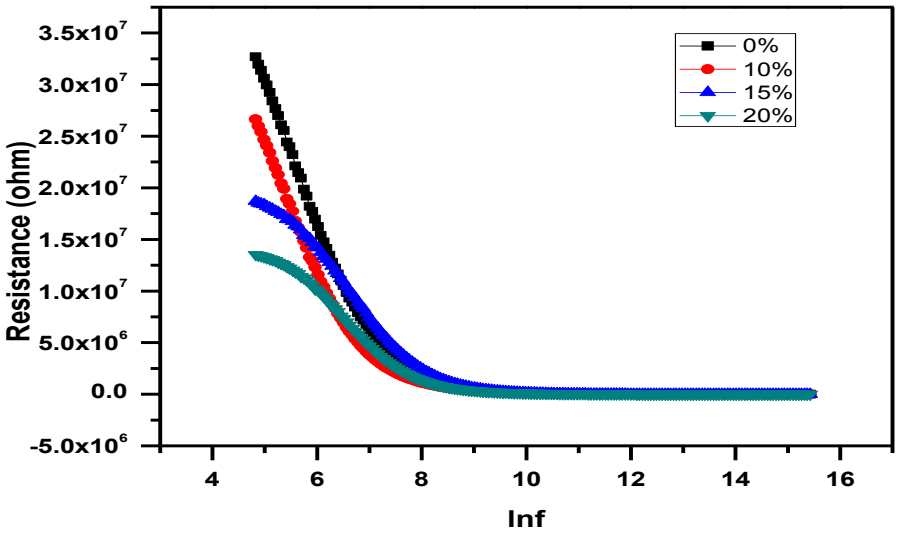

Fig. 4.21: Trend of resistance (real part of impedance) with frequency for $NiFe_2O_4$/CNFs nanohybrid as a function of CNFs contents (weight %).

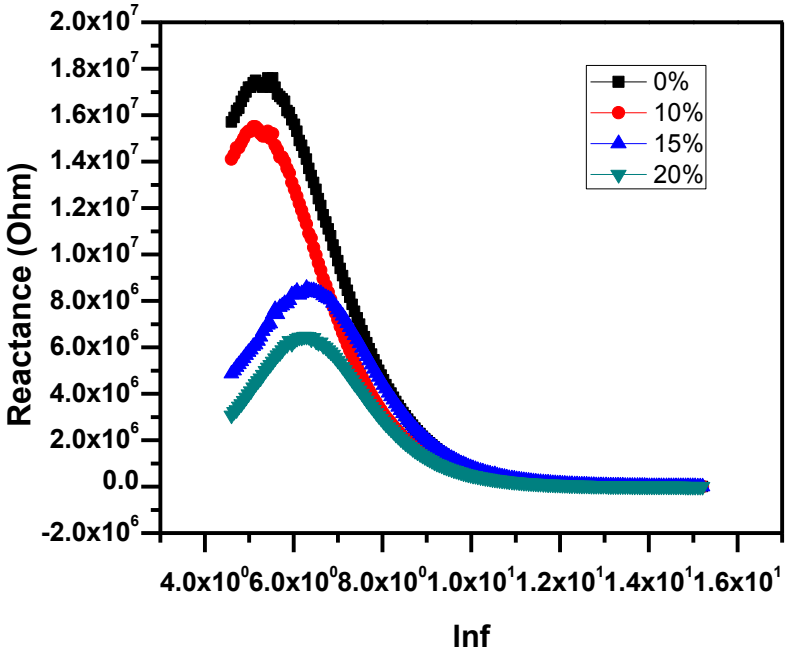

Fig. 4.22: Trend of reactance (imaginary part of impedance) with frequency for $NiFe_2O_4$/CNFs nanohybrid as a function of CNFs contents (weight %).

This trend of decreasing impedance with increasing frequency can be explained on the basis of space charge polarization, due to which hopping of electrons do not follow the fluctuating AC electric field. As frequency increases, this effect of space charge polarization decreases, due to which impedance values become constant at higher frequencies.

Fig. 4.23 shows the cole-cole plot of pure $NiFe_2O_4$ and $NiFe_2O_4$ /CNF nanohybrid with 10%, 15% and 20% CNFs concentration. The plot shows the incomplete semicircular arcs. The semicircular arcs towards the low-frequency region is due to the grain boundary conduction and that towards the high-frequency region is due to the grain conduction [78]. Fig. 4.23 shows the semicircular arcs towards low frequency region which means the resistance is only due to the grain boundary conduction while plot do not show any semicircular arc towards high frequency region which refers to the fact that there is possibly no contribution of grains conduction . The lowest grain boundary resistance (Rgb) is shown by pure $NiFe_2O_4$ and highest grain boundary resistance (Rgb) is shown by 20% $NiFe_2O_4$/CNF Nano hybrid as shown in Fig. 4.23. The charge transfer and electron-hole separation happens fastly at the interfaces between CNFs and ferrite [52], these

interfaces increase along with the increase in percentage of CNFs [42], which lowers the grain boundary resistance. This phenomenon can be attributed to the conductive network of CNFs [79], the interfaces between CNFs and ferrite acts as parallel plate capacitor, which facilitates the hopping of electrons, thus decreasing grain boundary resistance [80]. Thus it can be said that CNFs possess the great potential of enhancing charge transfer and electron–hole separation by reducing the grain boundary resistance.

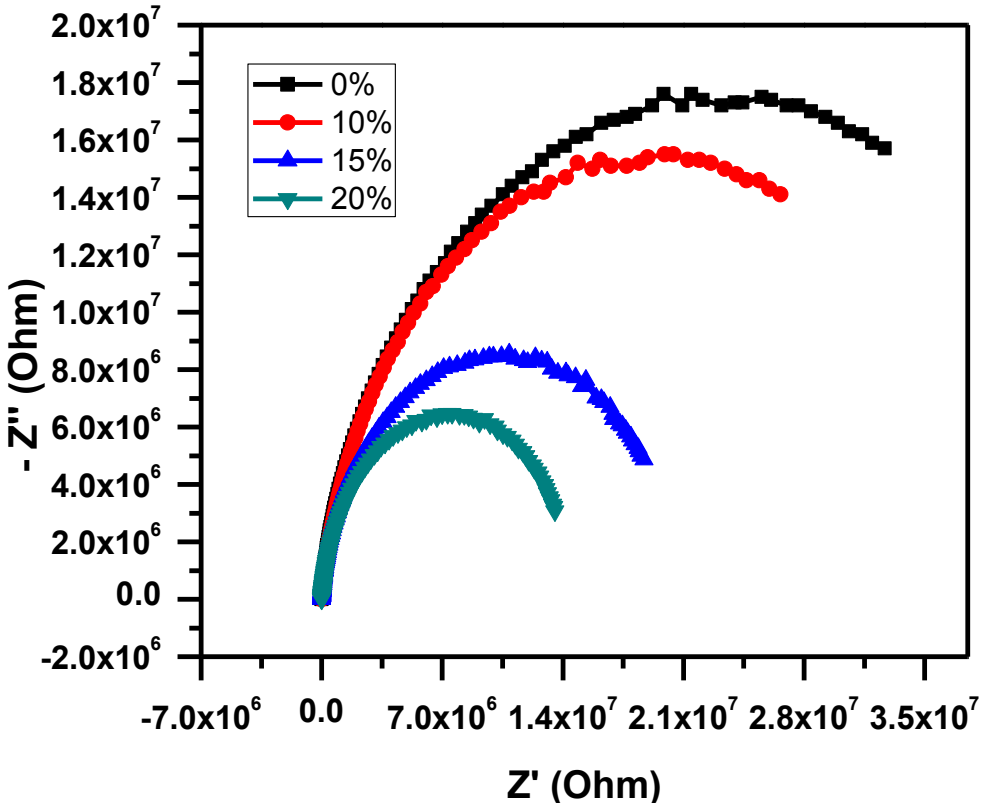

Fig. 4.23: Nyquist or Cole-Cole plot of the impedance for $NiFe_2O_4$/CNFs nanohybrid as a function of CNFs contents (weight %).

Conclusions:

Now a days, there is lots of energy crisis in the whole world, particularly in developing countries like Pakistan. To meet energy needs, most of the global countries rely on fossil fuels, due to which environment is deteriorating day by day. This prevailing situation of energy crisis compels the scientists to focus on this current issue.

To protect Earth's atmosphere, fossil fuel consumption will need to switch over to electric power but now a days electricity storage is a very big problem. Even capacitor has very low storage of charge. We need a sustainable energy system which can store huge amount of charge. So, we tried to design a material with the enhanced dielectric properties. Hence we synthesized Nickel ferrite / CNFs nanohybrid.

The work presented here shows the novel, facile and one step method of synthesizing $NiFe_2O_4$ /CNF Nano hybrid. The techniques used for characterization (XRD, SEM, LCR and impedance spectroscopy) showed the efficiency of the above described easy synthesis method and demonstrated the flawless and impurity less coating of $NiFe_2O_4$ on the CNFs surface without affecting the spinel structure of $NiFe_2O_4$.There was huge enhancement in dielectric properties and impedance values were considerably decreased due to the addition of CNFs. All the dielectric properties including dielectric constant, dielectric loss, tangent loss and AC conductivity showed enhancement with increment of percentage of added CNFs in nanohybid, proving CNFs to be potential partner for Nano hybrids of ferrites.

The massive enhancement in dielectric constant of up to 3.2×10^6 for 20% CNF hybrid is observed, which indicates the potential of the $NiFe_2O_4$ /CNF Nano hybrid for use in supercapacitors. The considerable decrease in impedance parameters proves the Nano hybrid to be highly recommended candidate for high frequency applications and microwave devices.

Future Work:

This nanohybrid can be further studied in following ways:

- Either by increasing percentage content of carbon nanofibers or by adding some suitable polymer into it.
- The addition of polymer can enhance its properties for various applications.
- This nanohybrid can also be characterized by several other techniques to discover its more potential applications in various fields.
- By further optimization this nanohybrid can bring revolution to optical, magnetism, electromagnetic, dielectric, microwave applications.

References:

[1] J. A. Barreto, W. O'Malley, M. Kubeil, B. Graham, H. Stephan, and L. Spiccia, "Nanomaterials: applications in cancer imaging and therapy," *Advanced Materials,* vol. 23, 2011.

[2] N. Chopra, V. G. Gavalas, L. G. Bachas, B. J. Hinds, and L. G. Bachas, "Functional One-Dimensional Nanomaterials: Applications in Nanoscale Biosensors," *Analytical Letters,* vol. 40, pp. 2067-2096, 2007.

[3] Q. A. Pankhurst, J. Connolly, S. K. Jones, and J. Dobson, "Applications of magnetic nanoparticles in biomedicine," *Journal of physics D: Applied physics,* vol. 36, p. R167, 2003.

[4] Q. Li, S. Mahendra, D. Y. Lyon, L. Brunet, M. V. Liga, D. Li*, et al.*, "Antimicrobial nanomaterials for water disinfection and microbial control: potential applications and implications," *Water research,* vol. 42, pp. 4591-4602, 2008.

[5] S. Hazra and N. Ghosh, "Preparation of nanoferrites and their applications," *Journal of nanoscience and nanotechnology,* vol. 14, pp. 1983-2000, 2014.

[6] M. A. Dar, V. Verma, S. Gairola, W. Siddiqui, R. K. Singh, and R. Kotnala, "Low dielectric loss of Mg doped Ni–Cu–Zn nano-ferrites for power applications," *Applied Surface Science,* vol. 258, pp. 5342-5347, 2012.

[7] P. Mathur, A. Thakur, J. Lee, and M. Singh, "Sustained electromagnetic properties of Ni–Zn–Co nanoferrites for the high-frequency applications," *Materials Letters,* vol. 64, pp. 2738-2741, 2010.

[8] V. Polshettiwar, M. N. Nadagouda, and R. S. Varma, "The synthesis and applications of a micro-pine-structured nanocatalyst," *Chemical Communications,* pp. 6318-6320, 2008.

[9] G. Herzer, "Nanocrystalline soft magnetic materials," *Physica Scripta,* vol. 1993, p. 307, 1993.

[10] A. Makino, T. Hatanai, A. Inoue, and T. Masumoto, "Nanocrystalline soft magnetic Fe-MB (M= Zr, Hf, Nb) alloys and their applications," *Materials Science and Engineering: A,* vol. 226, pp. 594-602, 1997.

[11] K. Buschow, "New developments in hard magnetic materials," *Reports on Progress in Physics,* vol. 54, p. 1123, 1991.

[12] W. D. Callister and D. G. Rethwisch, *Materials science and engineering* vol. 5: John Wiley & Sons NY, 2011.

[13] F. Morin, "Oxides which show a metal-to-insulator transition at the Neel temperature," *Physical Review Letters,* vol. 3, p. 34, 1959.

[14] S. Bedanta and W. Kleemann, "Supermagnetism," *Journal of Physics D: Applied Physics,* vol. 42, p. 013001, 2008.

[15] D. S. Mathew and R.-S. Juang, "An overview of the structure and magnetism of spinel ferrite nanoparticles and their synthesis in microemulsions," *Chemical Engineering Journal,* vol. 129, pp. 51-65, 2007.

[16] N. A. Spaldin and N. D. Mathur, "Magnetic Materials: Fundamentals and Device Applications," *Physics Today,* vol. 56, pp. 62-63, 2003.

[17] M. A. Gabal, "Non-isothermal decomposition of NiC2O4–FeC2O4 mixture aiming at the production of NiFe2O4," *Journal of Physics and Chemistry of Solids,* vol. 64, pp. 1375-1385, 2003.

[18] A. Alarifi, N. M. Deraz, and S. Shaban, "Structural, morphological and magnetic properties of NiFe2O4 nano-particles," *Journal of Alloys and Compounds,* vol. 486, pp. 501-506, 2009.

[19] D.-y. Li, Y.-k. Sun, P.-z. Gao, X.-l. Zhang, and H.-l. Ge, "Structural and magnetic properties of nickel ferrite nanoparticles synthesized via a template-assisted sol–gel method," *Ceramics International,* vol. 40, pp. 16529-16534, 2014.

[20] M. G. Naseri, E. B. Saion, H. A. Ahangar, M. Hashim, and A. H. Shaari, "Simple preparation and characterization of nickel ferrite nanocrystals by a thermal treatment method," *Powder Technology,* vol. 212, pp. 80-88, 2011.

[21] R. B. Kamble and V. L. Mathe, "Nanocrystalline nickel ferrite thick film as an efficient gas sensor at room temperature," *Sensors and Actuators B: Chemical,* vol. 131, pp. 205-209, 2008.

[22] J. L. Gunjakar, A. M. More, V. R. Shinde, and C. D. Lokhande, "Synthesis of nanocrystalline nickel ferrite (NiFe2O4) thin films using low temperature modified chemical method," *Journal of Alloys and Compounds,* vol. 465, pp. 468-473, 2008.

[23] S. E. Jacobo, M. Arana, and P. G. Bercoff, "Gadolinium substitution effect on the thermomagnetic properties of Ni ferrite ferrofluids," *Journal of Magnetism and Magnetic Materials,* vol. 415, pp. 30-34, 2016.

[24] A. S. Albuquerque, M. V. C. Tolentino, J. D. Ardisson, F. C. C. Moura, R. de Mendonça, and W. A. A. Macedo, "Nanostructured ferrites: Structural analysis and catalytic activity," *Ceramics International,* vol. 38, pp. 2225-2231, 2012.

[25] Y. Cheng, Y. Zheng, Y. Wang, F. Bao, and Y. Qin, "Synthesis and magnetic properties of nickel ferrite nano-octahedra," *Journal of Solid State Chemistry,* vol. 178, pp. 2394-2397, 2005.

[26] S. Joshi, M. Kumar, S. Chhoker, G. Srivastava, M. Jewariya, and V. N. Singh, "Structural, magnetic, dielectric and optical properties of nickel ferrite nanoparticles synthesized by co-precipitation method," *Journal of Molecular Structure,* vol. 1076, pp. 55-62, 2014.

[27] K. Maaz, S. Karim, A. Mumtaz, S. K. Hasanain, J. Liu, and J. L. Duan, "Synthesis and magnetic characterization of nickel ferrite nanoparticles prepared by co-precipitation route," *Journal of Magnetism and Magnetic Materials,* vol. 321, pp. 1838-1842, 2009.

[28] M. Asghari, A. Ghasemi, E. Paimozd, and A. Morisako, "Evaluation of microwave and magnetic properties of substituted SrFe12O19 and substituted SrFe12O19/multi-walled carbon nanotubes nanocomposites," *Materials Chemistry and Physics,* vol. 143, pp. 161-166, 2013.

[29] A. Maqsood and K. Khan, "Structural and microwave absorption properties of Ni(1−x)Co(x)Fe2O4 (0.0≤x≤0.5) nanoferrites synthesized via co-precipitation route," *Journal of Alloys and Compounds,* vol. 509, pp. 3393-3397, 2011.

[30] H. Li, H.-z. Wu, and G.-x. Xiao, "Effects of synthetic conditions on particle size and magnetic properties of NiFe 2 O 4," *Powder Technology,* vol. 198, pp. 157-166, 2010.

[31] P. Sivakumar, R. Ramesh, A. Ramanand, S. Ponnusamy, and C. Muthamizhchelvan, "Preparation and properties of nickel ferrite (NiFe2O4) nanoparticles via sol–gel auto-combustion method," *Materials Research Bulletin,* vol. 46, pp. 2204-2207, 2011.

[32] L. Guo, X. Shen, X. Meng, and Y. Feng, "Effect of Sm 3+ ions doping on structure and magnetic properties of nanocrystalline NiFe 2 O 4 fibers," *Journal of Alloys and Compounds,* vol. 490, pp. 301-306, 2010.

[33] B. Randhawa, J. Singh, H. Kaur, and M. Kaur, "Preparation of nickel ferrite from thermolysis of nickel tris (malonato) ferrate (III) heptahydrate precursor," *Ceramics International,* vol. 36, pp. 1993-1996, 2010.

[34] P. Sivakumar, R. Ramesh, A. Ramanand, S. Ponnusamy, and C. Muthamizhchelvan, "Preparation of sheet like polycrystalline NiFe 2 O 4 nanostructure with PVA matrices and their properties," *Materials Letters,* vol. 65, pp. 1438-1440, 2011.

[35] L. Chen, H. Dai, Y. Shen, and J. Bai, "Size-controlled synthesis and magnetic properties of NiFe 2 O 4 hollow nanospheres via a gel-assistant hydrothermal route," *Journal of Alloys and Compounds,* vol. 491, pp. L33-L38, 2010.

[36] C. Bousquet-Berthelin, D. Chaumont, and D. Stuerga, "Flash microwave synthesis of trevorite nanoparticles," *Journal of Solid State Chemistry,* vol. 181, pp. 616-622, 2008.

[37] S. Patange, S. E. Shirsath, S. Jadhav, K. Lohar, D. Mane, and K. Jadhav, "Rietveld refinement and switching properties of Cr 3+ substituted NiFe 2 O 4 ferrites," *Materials Letters,* vol. 64, pp. 722-724, 2010.

[38] J. Jiang, L. Ai, and L. Li, "Multifunctional polypyrrole/strontium hexaferrite composite microspheres: preparation, characterization, and properties," *The Journal of Physical Chemistry B,* vol. 113, pp. 1376-1380, 2009.

[39] S. Briceño, P. Silva, W. Molina, W. Brämer-Escamilla, O. Alcalá, and E. Cañizales, "Magnetic properties of NiFe2O4/carbon nanofibers from Venezuelan petcoke," *Journal of Magnetism and Magnetic Materials,* vol. 381, pp. 10-13, 2015.

[40] S. Tyagi, H. B. Baskey, R. C. Agarwala, V. Agarwala, and T. C. Shami, "Development of hard/soft ferrite nanocomposite for enhanced microwave absorption," *Ceramics International,* vol. 37, pp. 2631-2641, 2011.

[41] P. Sahoo, R. G. Shrestha, L. K. Shrestha, J. P. Hill, T. Takei, and K. Ariga, "Surface Oxidized Carbon Nanotubes Uniformly Coated with Nickel Ferrite Nanoparticles," *Journal of Inorganic and Organometallic Polymers and Materials,* vol. 26, pp. 1301-1308, 2016.

[42] G. G. Tibbetts, M. L. Lake, K. L. Strong, and B. P. Rice, "A review of the fabrication and properties of vapor-grown carbon nanofiber/polymer composites," *Composites Science and Technology,* vol. 67, pp. 1709-1718, 2007.

[43] Y. Li, S. Bae, A. Sakoda, and M. Suzuki, "Formation of vapor grown carbon fibers with sulfuric catalyst precursors and nitrogen as carrier gas," *Carbon,* vol. 39, pp. 91-100, 2001.

[44] L. Radushkevich and V. Lukyanovich, "About the structure of carbon formed by thermal decomposition of carbon monoxide on iron substrate," *J. Phys. Chem.(Moscow),* vol. 26, pp. 88-95, 1952.

[45] A. Oberlin, M. Endo, and T. Koyama, "Filamentous growth of carbon through benzene decomposition," *Journal of crystal growth,* vol. 32, pp. 335-349, 1976.

[46] G. G. Tibbetts, "Lengths of carbon fibers grown from iron catalyst particles in natural gas," *Journal of Crystal Growth,* vol. 73, pp. 431-438, 1985.

[47] L. Guadagno, M. Raimondo, V. Vittoria, L. Vertuccio, K. Lafdi, B. De Vivo*, et al.*, "The role of carbon nanofiber defects on the electrical and mechanical properties of CNF-based resins," *Nanotechnology,* vol. 24, p. 305704, 2013.

[48] L. Rassaei, M. Sillanpää, M. J. Bonné, and F. Marken, "Carbon nanofiber–polystyrene composite electrodes for electroanalytical processes," *Electroanalysis,* vol. 19, pp. 1461-1466, 2007.

[49] K.-Y. Park, J.-H. Han, S.-B. Lee, J.-B. Kim, J.-W. Yi, and S.-K. Lee, "Fabrication and electromagnetic characteristics of microwave absorbers containing carbon nanofibers and NiFe particles," *Composites Science and Technology,* vol. 69, pp. 1271-1278, 2009.

[50] J. Jacob and M. Abdul Khadar, "VSM and Mössbauer study of nanostructured hematite," *Journal of Magnetism and Magnetic Materials,* vol. 322, pp. 614-621, 2010.

[51] L. Fernández-García, M. Suárez, J. Luis Menéndez, C. Pecharromán, R. Torrecillas, P. Y. Peretyagin*, et al.*, "Antiresonance in (Ni,Zn) ferrite-carbon nanofibres nanocomposites," *Materials Research Express,* vol. 2, p. 055003, 2015.

[52] L. Feng, N. Xie, and J. Zhong, "Carbon nanofibers and their composites: a review of synthesizing, properties and applications," *Materials,* vol. 7, pp. 3919-3945, 2014.

[53] Y. Rangom, X. Tang, and L. F. Nazar, "Carbon Nanotube-Based Supercapacitors with Excellent ac Line Filtering and Rate Capability via Improved Interfacial Impedance," *ACS Nano,* vol. 9, pp. 7248-7255, 2015/07/28 2015.

[54] R. Balasubramaniam, *Callister'S Materials Science And Engineering: Indian Adaptation (W/Cd)*: John Wiley & Sons, 2009.

[55] N. Glumac, B. H. Kear, G. Skandan, and Y. Chen, "Combustion flame synthesis of nanophase materials," ed: Google Patents, 1999.
[56] R. P. Bagwe, C. Yang, L. R. Hilliard, and W. Tan, "Optimization of Dye-Doped Silica Nanoparticles Prepared Using a Reverse Microemulsion Method," *Langmuir,* vol. 20, pp. 8336-8342, 2004/09/01 2004.
[57] E. H. Kim, H. S. Lee, B. K. Kwak, and B.-K. Kim, "Synthesis of ferrofluid with magnetic nanoparticles by sonochemical method for MRI contrast agent," *Journal of Magnetism and Magnetic Materials,* vol. 289, pp. 328-330, 2005.
[58] Y. Zhang, Z. Yang, D. Yin, Y. Liu, C. Fei, R. Xiong*, et al.*, "Composition and magnetic properties of cobalt ferrite nano-particles prepared by the co-precipitation method," *Journal of Magnetism and Magnetic Materials,* vol. 322, pp. 3470-3475, 2010.
[59] H. Xie, G. Hu, K. Du, Z. Peng, and Y. Cao, "An improved continuous co-precipitation method to synthesize LiNi 0.80 Co 0.15 Al 0.05 O 2 cathode material," *Journal of Alloys and Compounds,* vol. 666, pp. 84-87, 2016.
[60] T. Eicher, S. Hauptmann, and A. Speicher, *The Chemistry of Heterocycles: Structures, Reactions, Synthesis, and Applications 3rd*: John Wiley & Sons, 2013.
[61] M. Z. Khan, I. H. Gul, H. Anwar, S. Ameer, A. N. Khan, A. A. Khurram*, et al.*, "Massive dielectric properties enhancement of MWCNTs/CoFe2O4 nanohybrid for super capacitor applications," *Journal of Magnetism and Magnetic Materials,* vol. 424, pp. 382-387, 2017.
[62] V. Klang, N. B. Matsko, C. Valenta, and F. Hofer, "Electron microscopy of nanoemulsions: an essential tool for characterisation and stability assessment," *Micron,* vol. 43, pp. 85-103, 2012.
[63] P. M. Chaikin and T. C. Lubensky, *Principles of condensed matter physics*: Cambridge university press, 2000.
[64] R. P. Scott, "Analytical Spectroscopy," ed.
[65] G. E. Lloyd, "Atomic number and crystallographic contrast images with the SEM: a review of backscattered electron techniques," *Mineralogical Magazine,* vol. 51, pp. 3-19, 1987.
[66] Y. Leng, *Materials characterization: introduction to microscopic and spectroscopic methods*: John Wiley & Sons, 2009.
[67] M. Raghasudha, D. Ravinder, and P. Veerasomaiah, "Influence of Cr³⁺ Ion on the Dielectric Properties of Nano Crystalline Mg-Ferrites Synthesized by Citrate-Gel Method," *Materials Sciences and Applications,* vol. 04, pp. 432-438, 2013.
[68] S. Briceño, W. Brämer-Escamilla, P. Silva, J. García, H. Del Castillo, M. Villarroel*, et al.*, "NiFe2O4/activated carbon nanocomposite as magnetic material from petcoke," *Journal of Magnetism and Magnetic Materials,* vol. 360, pp. 67-72, 2014.
[69] Q. Zhang, M. Zhu, Q. Zhang, Y. Li, and H. Wang, "Synthesis and characterization of carbon nanotubes decorated with manganese–zinc ferrite nanospheres," *Materials Chemistry and Physics,* vol. 116, pp. 658-662, 2009.
[70] M. Abdel Salam, M. A. Gabal, and A. Y. Obaid, "Preparation and characterization of magnetic multi-walled carbon nanotubes/ferrite nanocomposite and its application for the removal of aniline from aqueous solution," *Synthetic Metals,* vol. 161, pp. 2651-2658, 2012.
[71] M. Sajjia, M. Oubaha, M. Hasanuzzaman, and A. Olabi, "Developments of cobalt ferrite nanoparticles prepared by the sol–gel process," *Ceramics International,* vol. 40, pp. 1147-1154, 2014.
[72] R. Melo, F. Silva, K. Moura, A. de Menezes, and F. Sinfrônio, "Magnetic ferrites synthesised using the microwave-hydrothermal method," *Journal of Magnetism and Magnetic Materials,* vol. 381, pp. 109-115, 2015.

[73] K. Rao, G. Choudary, K. Rao, and C. Sujatha, "Structural and Magnetic Properties of Ultrafine CoFe 2 O 4 Nanoparticles," *Procedia Materials Science,* vol. 10, pp. 19-27, 2015.

[74] A. K. Nikumbh, R. A. Pawar, D. V. Nighot, G. S. Gugale, M. D. Sangale, M. B. Khanvilkar*, et al.*, "Structural, electrical, magnetic and dielectric properties of rare-earth substituted cobalt ferrites nanoparticles synthesized by the co-precipitation method," *Journal of Magnetism and Magnetic Materials,* vol. 355, pp. 201-209, 2014.

[75] R. L. Poveda and N. Gupta, *Carbon nanofiber reinforced polymer composites*, 2015.

[76] C. Murugesan, M. Perumal, and G. Chandrasekaran, "Structural, dielectric and magnetic properties of cobalt ferrite prepared using auto combustion and ceramic route," *Physica B: Condensed Matter,* vol. 448, pp. 53-56, 2014.

[77] E. Pervaiz and I. Gul, "Enhancement of electrical properties due to Cr 3+ substitution in Co-ferrite nanoparticles synthesized by two chemical techniques," *Journal of Magnetism and Magnetic Materials,* vol. 324, pp. 3695-3703, 2012.

[78] N. Ponpandian, P. Balaya, and A. Narayanasamy, "Electrical conductivity and dielectric behaviour of nanocrystalline NiFe2O4 spinel," *Journal of Physics: Condensed Matter,* vol. 14, p. 3221, 2002.

[79] E. Hammel, X. Tang, M. Trampert, T. Schmitt, K. Mauthner, A. Eder*, et al.*, "Carbon nanofibers for composite applications," *Carbon,* vol. 42, pp. 1153-1158, 2004.

[80] S. A. Soomro, I. H. Gul, M. Z. Khan, H. Naseer, and A. N. Khan, "Dielectric properties evaluation of NiFe 2 O 4/MWCNTs nanohybrid for microwave applications prepared via novel one step synthesis," *Ceramics International,* 2016.